universität wien

DIPLOMARBEIT / DIPLOMA THESIS

Titel der Diplomarbeit / Title of the Diploma Thesis

„Quantification of the open chain content of aldoses *via* kinetics of ABAO-adduct formation“

verfasst von / submitted by

Alexander Reichetseder

angestrebter akademischer Grad / in partial fulfilment of the requirements for the degree of

Magister der Pharmazie (Mag.pharm.)

Wien, 2018/ Vienna, 2018

Studienkennzahl lt. Studienblatt / degree programme code as it appears on the student record sheet:	A 449
Studienrichtung lt. Studienblatt / degree programme as it appears on the student record sheet:	Diplomstudium Pharmazie
Betreut von / Supervisor:	Univ.-Prof. Dipl.-Ing. Dr. Marko D. Mihovilovic

Acknowledgements

First, I want to thank Univ.-Prof. Dipl.-Ing. Dr. Marko D. Mihovilovic for the opportunity to conduct my diploma thesis in his research group.

Special thanks go to Dipl.-Ing. Dr. Christian Stanetty for his supervision and his motivating words through the whole thesis.

I want to thank Dipl.-Ing. Markus Draskovits BSc and Hubert Kalaus BSc for helping me in the laboratory with my practical work.

Special thanks to the whole research group for the nice atmosphere and for inputs during the synthesis seminars.

Special thanks to ao. Univ.-Prof. Mag. Dr. Helmut Spreitzer for making this thesis possible as inter-university project.

Finally, I want to thank my family, my friends and my colleagues for supporting me and helping me being the person who I am right now.

Abbreviations

ABAO	2-Aminobenzamidoxime
d	doublet (NMR)
D_2O	deuterium oxide
DCM	dichloromethane
DMSO	dimethyl sulfoxide
DMSO-d_6	deuterated dimethyl sulfoxide
dd	doublet of doublets (NMR)
dt	doublet of triplets (NMR)
equiv.	equivalent
Et_2O	diethyl ether
EtOAc	ethyl acetate
EtOH	ethanol
iPrOH	*iso*-propanol
J	coupling constant (NMR)
LP	light petroleum
m	multiplet (NMR)
MeCN	acetonitrile
MeOH	methanol
NaOAc	sodium acetate
NH_4OAc	ammonium acetate
NMR	Nuclear Magnetic Resonance
ppm	parts per million
R_f	retention factor (TLC)
s	singlet (NMR)
TLC	Thin Layer Chromatography

Table of contents

1 Introduction

1.1 Mutarotation

If a crystalline sugar – aldose or ketose – is dissolved in water, a change of optical rotation can be observed until a constant value is reached. This was discovered by Augustin-Pierre Dubrunfaut in 1846 when he found that the specific rotation of freshly dissolved glucose was twice as high from that value which was published earlier. Therefore, he called this phenomenon “birotation”, which is known as mutarotation today[1].

The reason for this behaviour of sugars is that they are hardly available as an open chain, but mostly available in cyclic forms, so called hemiacetals. The hydroxy group at C5, for example, binds to the aldehyde carbon, a new chiral centre and two epimers are formed: α- and β-pyranose. To form a furanose, the oxygen at C4 binds to C1 instead of C5. Furanoses and Pyranoses are in equilibrium with the open chain form, but there is significantly more cyclic form than aldehyde available. Glucose, for example, has a very low content of aldehyde (**Scheme 1**), in contrast to tetroses, which have a relatively high aldehyde content. In addition, the open chain form is partially hydrated in aqueous solution to form a hydrate.

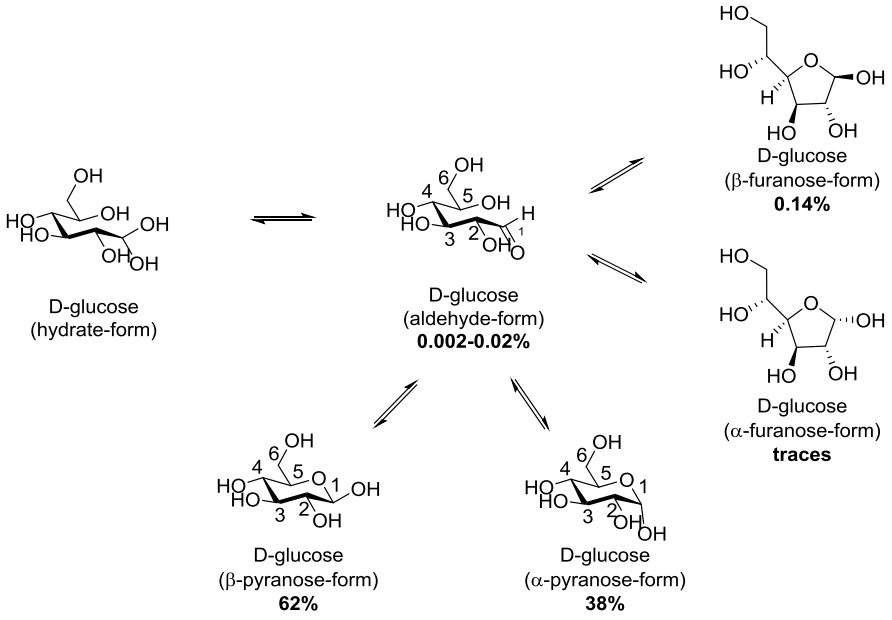

Scheme 1: Different forms of D-glucose.

1.2 Reactions with open chain form of reducing sugars

Although sugars are predominantly existing in the ring forms, also starting from the open chain form, various reactions can be performed.

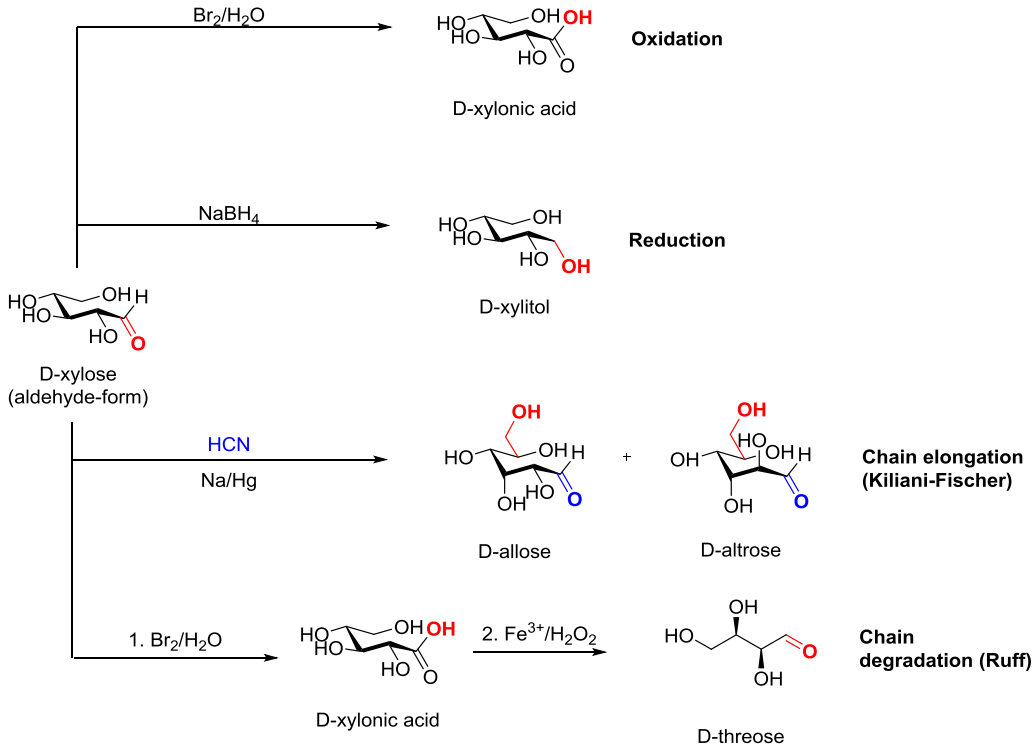

Scheme 2: Overview of possible reactions performed with the open chain form of aldoses.

As shown in **Scheme 2**, exemplifying xylose as the starting material, an oxidation of the aldehyde with bromine water can be done to get xylonic acid[2]. If xylitol is required, a reduction can be performed with $NaBH_4$ to obtain the corresponding sugar alcohol[3].

Furthermore, different chain elongations or degradations are described. If a chain elongation *via* Kiliani-Fischer is performed, starting from xylose as representative example, a mixture of allose and altrose is received[4][5]. Mechanistically, first, hydrogen cyanide adds as a nucleophile to the aldehyde to form a cyanohydrin. After hydrolysis of the nitrile furnishing a carboxylic acid, a reduction with sodium amalgam is carried out to obtain the aldehyde moiety of the elongated sugars.

If threose is wanted and xylose is the starting material, a chain degradation *via* Ruff is possible[6][7]. The aldehyde needs to be oxidized to a carboxylic acid first; afterwards the carboxylic acid is decarboxylated, and the sugar is shortened by one carbon.

1.3 Open chain content of aldoses

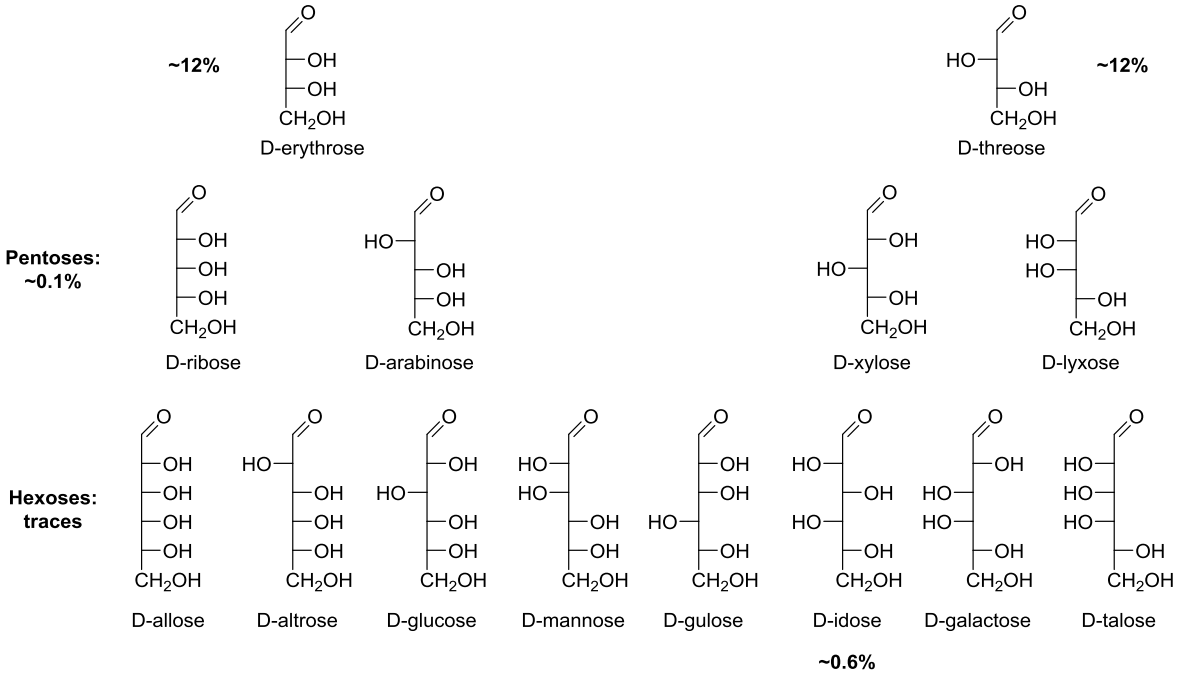

Scheme 3: Overview of the open chain content of aldoses.

As shown in **Scheme 3**, the open chain content of aldoses is quite variable. With about 12%, erythrose and threose are available as an open chain form to a high degree. While pentoses have already a low open chain content (around 0.1%), the open chain content of hexoses is, even lower, except for idose Due to low steric strain, the pyranose form of glucose is very stable and only low concentrations of open chain form are available. Idose has a relatively high concentration of open chain form, with all hydroxy groups in axial position (D-idose) and the axial hydroxymethyl (L-idose) both destabilizing the cycling form.

1.4 Methods to quantify different forms of sugars

Many different methods to measure the various forms of reducing sugars have been established in the past[8].

The first method to measure different forms of reducing sugars was polarimetry. However, this method has serious limitations as it is not able to measure the open chain form; additionally, if the cyclic forms – pyranose or furanose – are not known in the crystalline state, it does not give any useful results.

To measure the acyclic forms, different methods had to be used. Infrared spectroscopy had similar problems as NMR; circular dichroism was a promising method, however the values published with this method are often not exact.[8]

NMR spectroscopy is a much more powerful method and the first spectra of sugars were published as early as in 1961[8]. However, NMR is still not ideal to measure minor components as it is not sensitive enough to detect the aldehyde species in its low abundance, which is particularly true for ^{13}C-NMR that does not suffer from the many overlaps observed in ^{1}H-NMR of sugars. To approach this, $^{13}C_1$-enriched material was used, and even then the measurement itself is still time consuming. However, this method is still the "gold standard" and values taken from the tetroses were measured by NMR.

A different approach was reported by Dworkin et al. in 2000[9]. In this publication, a kinetic model was set up and reactions with urazole were performed (**Scheme 4**).

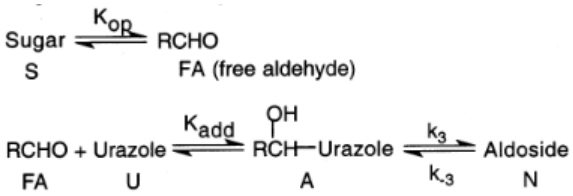

Scheme 4: Kinetic model of Dworkin et al. to measure the open chain form of aldoses.

K_{op} and K_{add} are in rapid equilibrium and k_3 is the slow step. The assumption of this approach was that K_{add} and k_3 are equal for all aldoses and the reaction rate depends on K_{op}, which is the free aldehyde content. This means that the relative stereochemistry of sugars is not taken into consideration and that, for example erythrose and threose should give a similar reaction rate due to their comparable open chain content.

Investigations that are described later in this thesis will show that this assumption is not quite exact for the method which is introduced and was refined in this thesis.

1.5 Quantification of aldehyde content by adduct formation and UV

A similar method was introduced by Kitov et al. in 2014[10]. This method was intended to modify aldehyde-terminated proteins (e.g. built-in quality control) originally, however, quite a few ideas were taken from this method and further developed towards the approach introduced in this thesis.

A reaction between 2-aminobenzamidoxime (ABAO) and an aldehyde is described to form an UV-active ABAO-adduct that can be followed by UV/vis (**Scheme 5**).

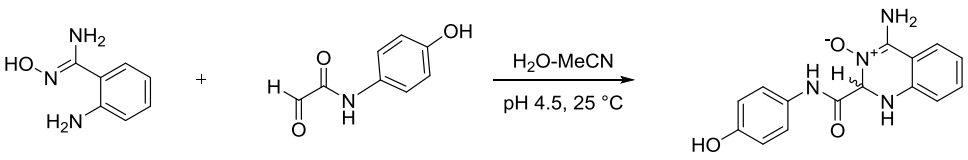

Scheme 5: Reaction between ABAO and aldehyde to form an UV-active adduct.

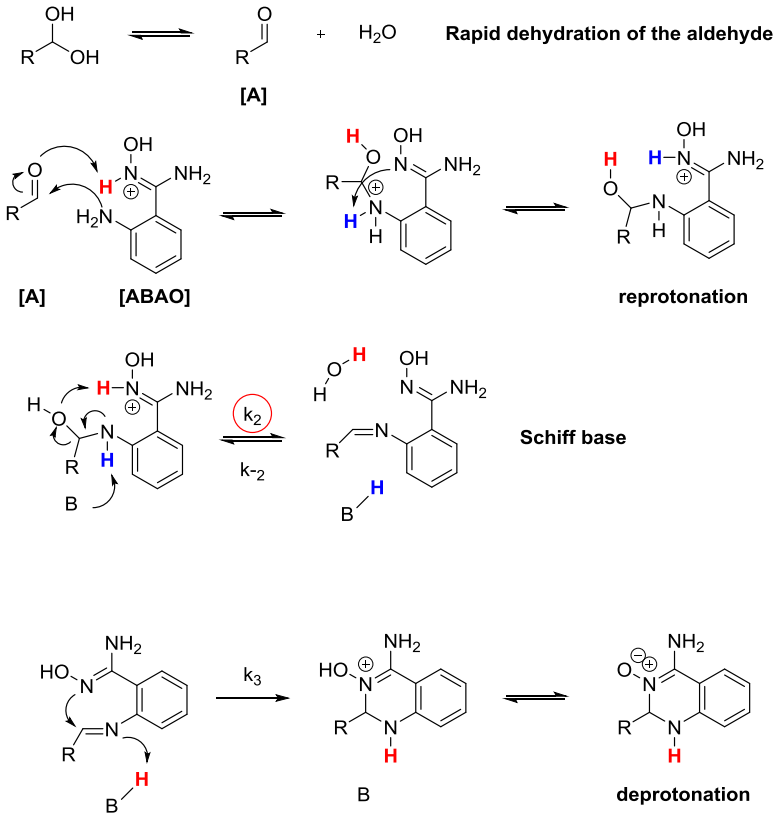

Scheme 6: Proposed mechanism of ABAO-adduct formation with the rate determining step k_2.

The proposed mechanism of ABAO adduct formation is shown in **Scheme 6**. First, the nitrogen attacks the aldehyde carbon and a carbinolamine is formed.

After carbinolamine elimination and Schiff base formation which is the rate determining step of this mechanism (**k_2**), a rapid intramolecular ring closure (**k_3**) and deprotonation leads to the final N-oxide structure.

Note that the dehydration of the aldehyde is not taken into consideration. This is known as a fast process and "[i]t should be safe to assume that production of aldehyde can be decoupled to pre-equilibrate rapidly" (Kitov et al, 2014)[10].

This method has been further developed by Prof. Mihovilovic's research group, in particular within a research project supervised by Dr. Florian Rudroff. In this project, a carboxylic acid was converted into an aldehyde enzymatically, and afterwards the reaction was performed with ABAO for assaying enzyme conversion during an

enzyme engineering campaign. With this method, the analytics of the aldehydes are autonomous of the moieties, consequently, enabling substrate-independent photometric conversion control: the absorption is proportional to the aldehyde content; a higher absorption means more aldehyde (**Scheme 7**).

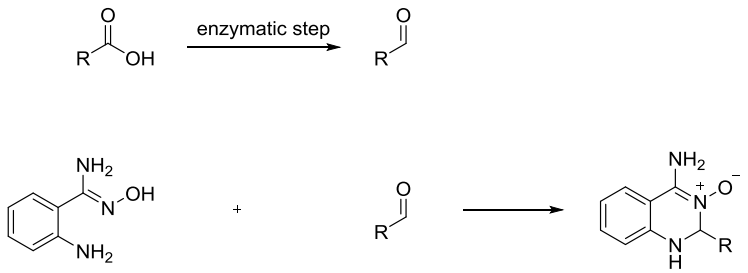

Scheme 7: Further developed method with regular aldehydes.

1.6 Aim of this thesis

The aim of this project was to find a method to measure the open chain content of reducing sugars which is easy to handle, time saving and does not need expensive equipment such as NMR.

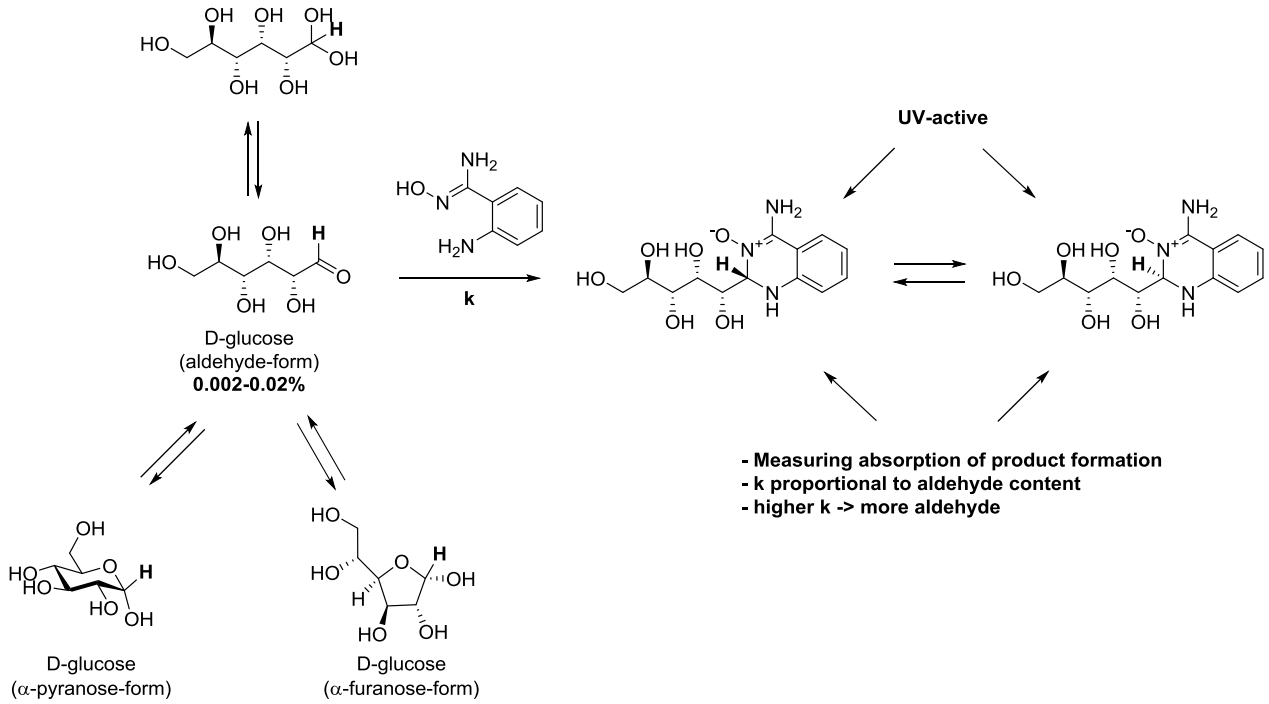

Scheme 8: Kinetic approach to measure the open chain content of aldoses.

As shown in **Scheme 8**, the method developed in this thesis is a kinetic approach where the open chain content is correlated to the rate of adduct formation that can easily be followed *via* UV-absorption.

The aldehyde form of an aldose reacts with 2-Aminobenzamidoxime to form an UV-active adduct and its absorption can be measured *via* UV/vis. According to our hypothesis, the rate ratio **k** is proportional to the aldehyde content of the sugar, which means the higher **k**, the more aldehyde is available. The goal of this thesis was to establish a reliable model to predict relative abundancies of the open chain content (or relative reactivity of the aldehyde function) in stereo-isomeric sugars in a straight-forward and reliable fashion.

2 Results and discussion

2.1 Initial assumption for the kinetic model

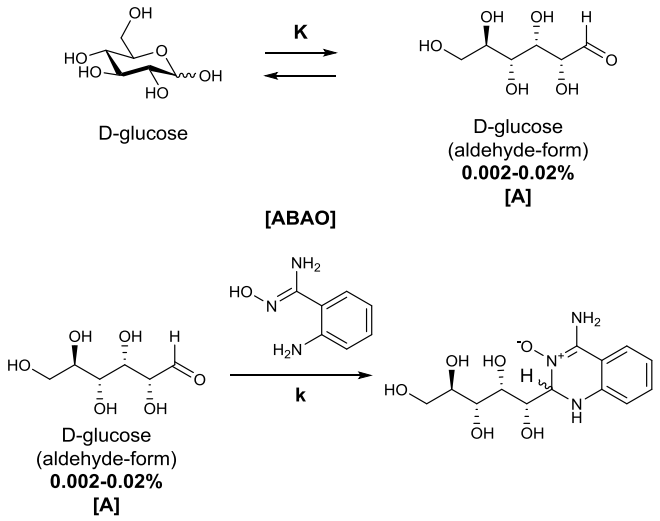

Scheme 9: Initial assumption: k is equal for all aldoses and the rate ratio depends on K.

Analogous to Kitov's assumption that hydrate liberation is very fast and can be ignored, also mutarotation was assumed to be sufficiently faster than adduct formation to ensure "steady-state-like" conditions.

In the early phase of this project, an assumption by Dworkin et al.[9] was taken into consideration. In this publication, a kinetic model was set up as well, but reactions with urazole instead of ABAO were performed. This assumption is shown in **Scheme 9**: the product formation **k** is equal for all aldoses; therefore, the observed rate constant would be directly proportional to **K**, which reflects the free aldehyde content.

Investigations that are described later in this thesis will show that this assumption is not quite exact for the method which is introduced in this thesis.

The reaction itself is a pseudo-first order reaction if significantly more ABAO is present than sugar (10:1), which means ABAO is available in excess and its concentration changes hardly over time. Instead of worrying about the aldehyde content (which is not known), the following equation can be made:

$-d[A]/dt = k_{app}[A]$ where $k_{app} = k_{real}[ABAO]_0$ [A] = aldehyde content

$k_{app} = [ABAO_0]*K*k_{real}$ $[ABAO_0]$ = starting ABAO conc.

$K*k_{real} = k_{app}/ABAO_0$ = **Total k**

k_{app} is the kinetic value if the curve is fitted *via* one phase association with the software *Prism* (or manually done in *Excel*) and total k is yielded when k_{app} is divided by the starting concentration of ABAO. Within this project, it was not possible to separate K (which is the equilibrium constant of the sugar's ring opening and closing) and k_{real}. Therefore, it is needed to know at least one of those values to determine the other one exactly.

2.2 Developing a standard procedure for determination of UV-curves with aldoses

As already mentioned, reactions with ABAO and aldehydes have already been performed in the past by Kitov et al and Prof. Mihovilovic's research group. However, instead of using sugar aldehydes, reactions with regular aldehydes have been performed. Therefore, the standard procedures from their experiments were the starting point for our optimisation of conditions for our task in a series of preliminary experiments with threose as prospective fast reacting and ribose as exemplary standard sugar (**Table 1**).

Table 1: Original and optimised conditions for UV-curve determination.

	Original conditions	**Optimised conditions for reducing sugars**
Concentration of aldehyde	1 mM aldehyde	4 mM sugar
Buffer	100 mM NaOAc buffer	100 mM NH_4OAc buffer
pH	pH = 4.5	pH = 4.5
Concentration of ABAO	Different equiv. of ABAO (5-30 mM)	40 mM ABAO

2.2.1 Finding the optimal conditions

With regular aldehydes and aldoses displaying a high open chain content, using the original concentrations (1 mM) is not a problem due to their high availability of aldehyde, which results in fast product formation. However, for aldoses which have a low availability of open chain content, higher concentrations of sugar and consequently ABAO were required to make the reaction sufficiently fast (**Scheme 10**).

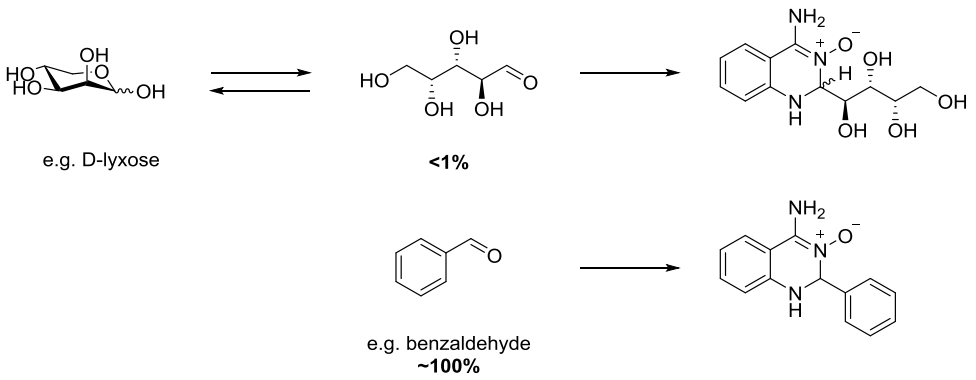

Scheme 10: Sugar aldehydes versus regular aldehydes reacting with ABAO.

2.2.2 Buffer

In early experiments with threose it seemed like that NH_4OAc buffer was faster than NaOAc (**Figure 1**). Therefore, and due to the volatility of NH_4OAc which would allow to obtain ABAO-adducts in a preparative way, NaOAc buffer was replaced by NH_4OAc buffer. Interestingly, there was no significant change in reaction rate with the pentoses depending whether NH_4OAc was used (**Table 2**).

Table 2: Comparison of k_{app} between NaOAc and NH_4OAc buffer.

Sugar	NaOAc buffer, k_{app} ($s^{-1}*10^{-4}$)	NH_4OAc buffer, k_{app} ($s^{-1}*10^{-4}$)
Lyxose	4.001	4.018
Ribose	3.388	3.375
Arabinose	2.008	1.890
Xylose	1.275	1.136

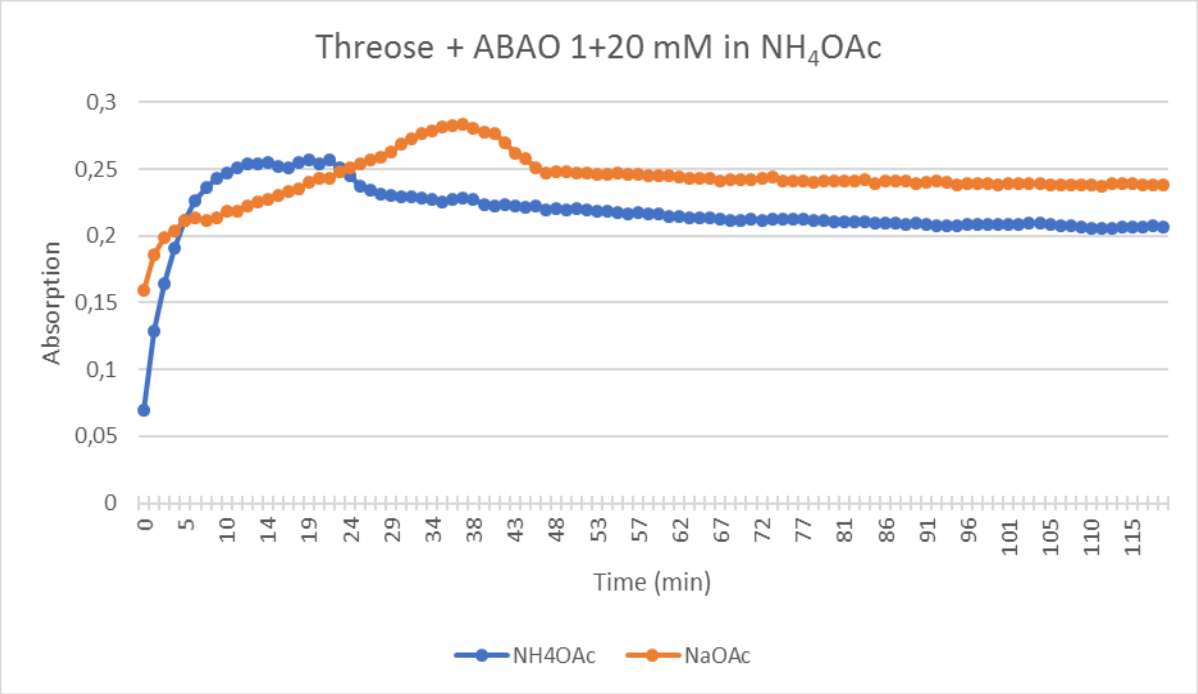

Figure 1: D-threose and ABAO reacting in different buffers with strange hump visible.

As shown in **Figure 1**, a strange hump is visible in the curves. Regarding the concentrations that were used in this measurement (1 mM sugar and 20 mM ABAO), this phenomenon seems to be a concentration issue as the hump disappears when the concentration is lowered. Other influences will be discussed later in this thesis.

2.2.3 Plate reader versus photometer

Most measurements were done with the plate reader. A big benefit of it is that it can measure multiple samples simultaneously. This saves a lot of time, as each sample can be determined in triplicates and theoretically, still up to 32 different samples are measurable by doing only one experiment. Furthermore, there is very little amount of sample solution needed to make a successful measurement, around 150-200 µl per well.

However, it is not possible to detect the first 30 to 60 seconds as the plate reader needs some time to start the measurement. Also note that pipetting multiple samples in triplicates takes some time. Furthermore, the wells cannot be covered so evaporation takes place in case of long measurements, and the temperature control is not so stable. Nevertheless, the reproducibility of the values measured by the plate reader is very high; this method is recommended if samples are measured with

absorption not rising so fast and for measuring multiple samples with one experiment.

The photometer on the other hand is more sensitive (requiring lower concentration), able to perform more measuring points within the same time and starts measuring immediately, however, a bigger sample size is needed (500 µl to 1 ml, depending on the cuvette). Furthermore, it is only able to measure one sample at the same time. This method is recommended if a particular exact measurement is needed or if the beginning of the measurement is decisive.

2.3 Synthesis of 2-Aminobenzamidoxime-derivatives

Table 3: Different ABAO-derivatives and their k[10].

ABAO-derivative	k ($m^{-1}s^{-1}$)
1a	0.003
1b	0.0016
1c	0.09
1d	0.72

The initial idea was to synthesize 3 different ABAO-derivatives to demonstrate slow, medium and fast product formation (**Table 3**) to be able to select the most appropriate derivative for the survey.

According to Kitov et al, 2014 there is a "relationship between the measured reaction rates and pKa of the corresponding protonated anilines […] and that a high basicity of the nitrogen is necessary to accelerate the Schiff base formation". ABAO-derivative **1a**, with the nitro moiety as a -M-substituent was reported to be the slowest one, whereas **1d** with the methoxy moiety as a +M-substituent is the fastest one.

Therefore, **1a** (slow) and **1c** (standard) were chosen to be synthesized, **1d** (fast) was already available in the lab. According to **Table 3**, their reaction rate should be sufficiently different to see a significant difference in product formation. At a later stage **1b** was prepared as alternative slow-performer.

However, it turned out that **1a** was not soluble in the buffer, so a solvent mixture with DMSO had to be made and lower concentrations had to be used to stay in the linear range of the UV-vis instrument. With that being said, the reaction slowed down so strongly nothing happened within a day. To keep the system as simple as possible, **1a** was replaced by **1b** as alternative slow performer, and solubility was not an issue at all with this derivative.

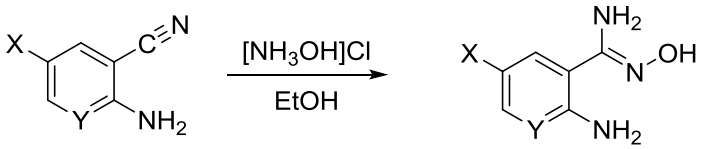

(X=NO_2, **Y**=C**), Ia**
(X=H, **Y**=N), **Ib**
(X=H, **Y**=C), **Ic**
(X=OMe, **Y**=C), **Id**

(X=NO_2, **Y**=C**), 1a**
(X=H, **Y**=N), **1b**
(X=H, **Y**=C), **1c**
(X=OMe, **Y**=C), **1d**

Scheme 11: Synthesis of 2-Aminobenzamidoxime-derivatives.

The 2-Aminobenzamidoxime-derivatives were prepared *via* procedures published in the literature (**Scheme 11**)[11].

To obtain a 2-Aminobenzamidoxime-deriative (**1a**, **1b**, **1c**), a mixture of the starting material, the corresponding 2-Aminobenzonitrile, $[NH_3OH]Cl$ and $NaHCO_3$ were dissolved in EtOH and refluxed. Hydroxylamine is formed in *situ* from $[NH_3OH]Cl$ and $NaHCO_3$ which adds to the nitrile to form an amidoxime (**Scheme 12**).

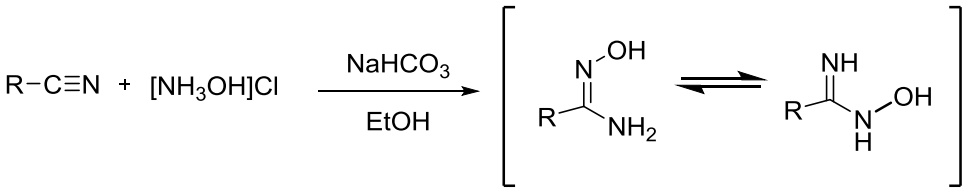

Scheme 12: Mechanism of amidoxime formation.

This step is identical with all 3 derivatives that were synthesized (**1a**, **1b**, **1c**). The obtained products can be purified *via* trituration in iPrOH (**1a**) or DCM/LP 1:1 (**1b**,**1c**).

2.4 Comparison of performance of ABAOs in the reaction with D-ribose and threose

Next the differently substituted ABAOs were subjected to reactions with D-ribose and D-threose to determine their relative reactivities.

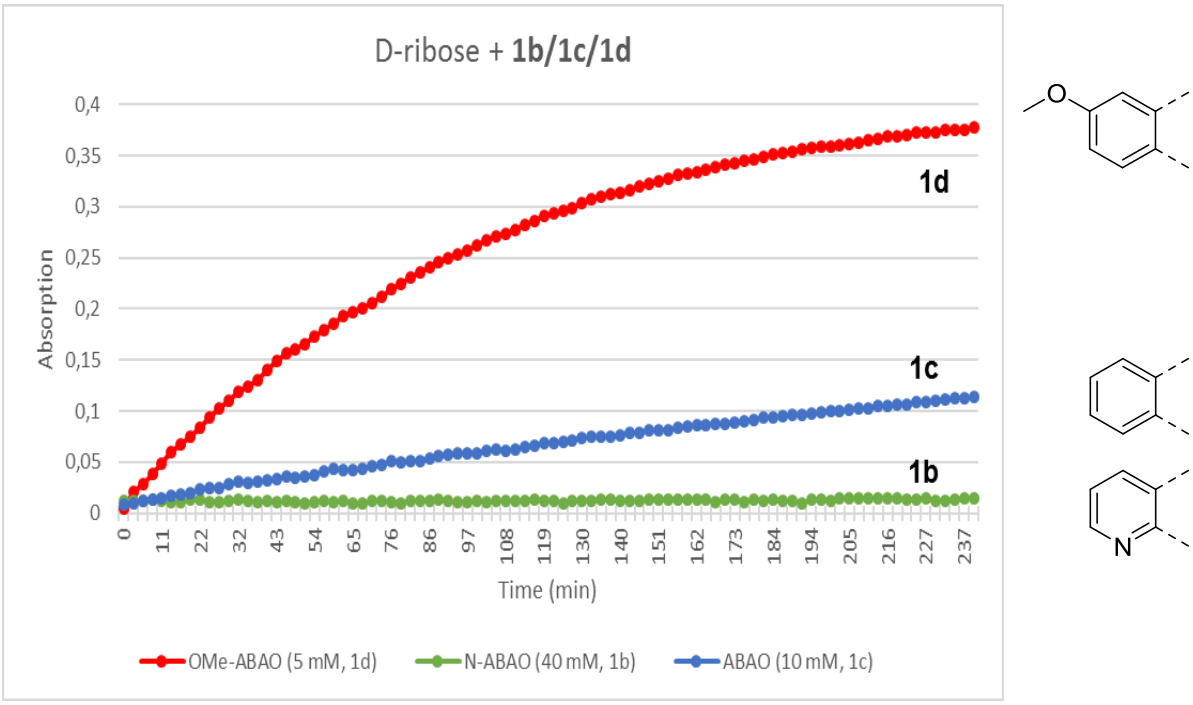

Figure 2: Different ABAO-derivatives reacting with D-ribose.

As shown in **Figure 2**, the reaction between **1d** and D-ribose was the fastest one, which was expected (**Table 4**) even under the lower concentration applied due to low solubility of **1d** in the buffer compared to **1b** and **1c**.

Table 4: Reactions between ABAO-derivatives and D-ribose and their kinetic data.

	k_{app} ($s^{-1}*10^{-4}$)	Total $k*10^{-3}$	Relative ratio
MeO-ABAO (1d)	1.6	32	4
ABAO (1c)	0.82	8.2	1
N-ABAO (1b)	-	-	-

The reaction with D-ribose and **1d** is 4 times faster compared to D-ribose and **1c**, and under the standard conditions it looked like **1b** was not reactive at all. However, in the experiment with threose as substantially faster sugar, product formation is observed (**Figure 4**) and a rate constant for comparison could be determined.

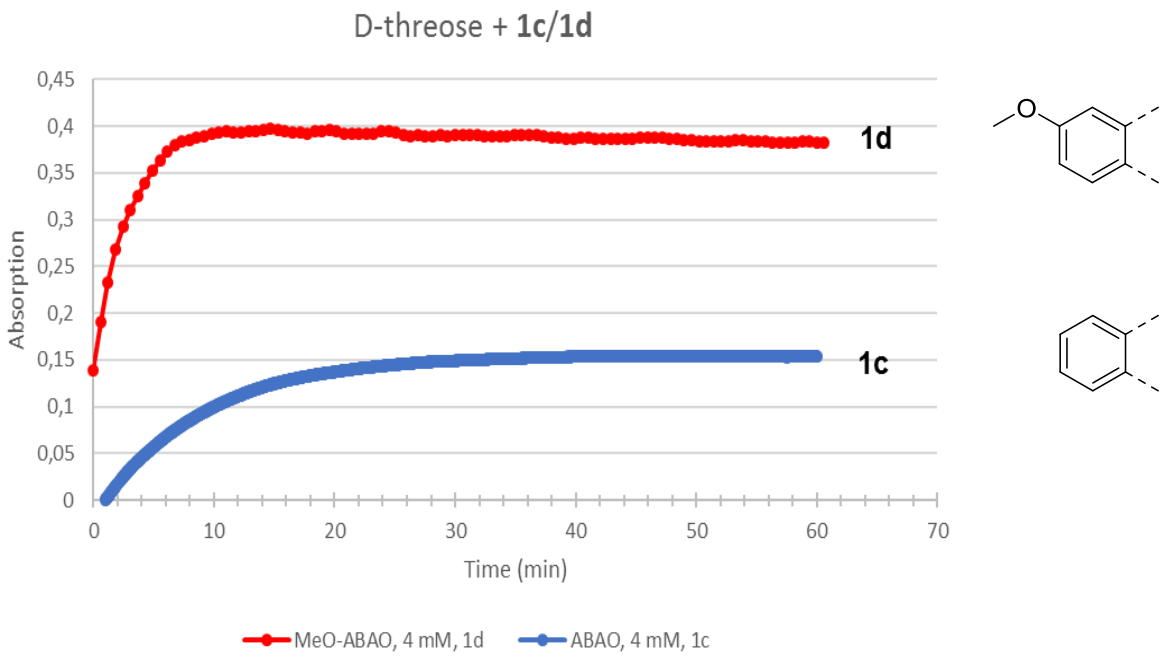

Figure 3: D-threose reacting with 1c/1d; no hump visible with 1c.

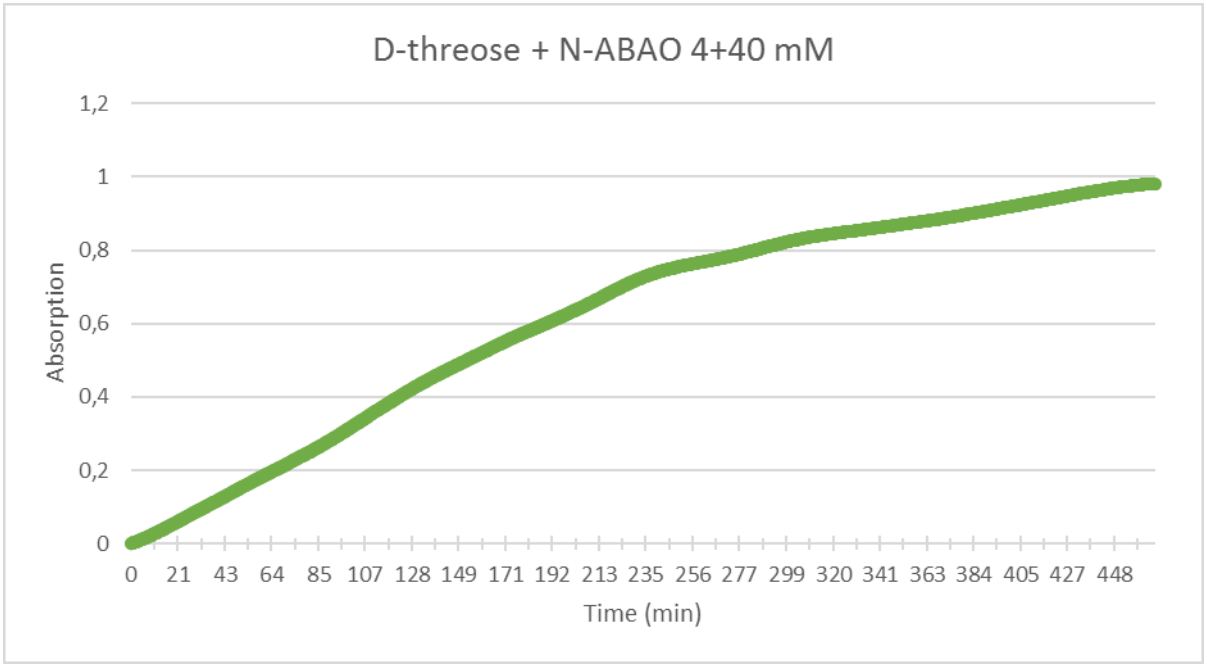

Figure 4: D-threose reacting with 1b.

Table 5: Reactions between ABAO-derivatives and D-threose and their kinetic data.

	k_{app} ($s^{-1}*10^{-5}$)	Total $k*10^{-3}$	Relative ratio
MeO-ABAO (1d)	675	1688	993
ABAO (1c)	190	483	284
N-ABAO (1b)	6.7	1.7	1

As shown in **Figure 4**, the product formation between **1b** and a sugar whose open chain content is high enough is clearly possible, however it seems like that adduct formation is still not completed after 8 hours, although threose, a sugar with a high open chain content is used. Product formation between D-threose and **1c**/**1d** is shown in **Figure 3**. With **1d**, product formation is finished after about 10 minutes, whereas with **1c** about 40 minutes are needed under these conditions.

According to **Table 5**, **1d** is 993 times and **1c** 284 times faster than **1b**. If **1c** and **1d** are compared to each other, **1d** is 3.5 times faster than **1c**, which is in good consistence to the ratio observed with ribose.

These measurements showed that the fast derivative (**1d**) is only operable in very low concentrations (around 5 mM), and the slow one (**1b**) has a very low reaction rate even with a fast sugar (e.g. threose). To make **1d** soluble in the buffer in higher concentrations, a mixture of DMSO and buffer is needed, and this would give different results, as DMSO changes the compositions of sugars[12]. Therefore, the medium derivative, **1c** was used exclusively for the rest of this project, as it has no solubility issues and it reacts still fast enough with most sugars to finish adduct formation.

2.5 Dependence of conversion from concentration

As already shown in **Figure 1**, a strange hump is visible in the curves. Regarding the concentrations that were used in this measurement (1 mM sugar and 20 mM ABAO), the hump disappears if the concentration is lowered (**Figure 5**).

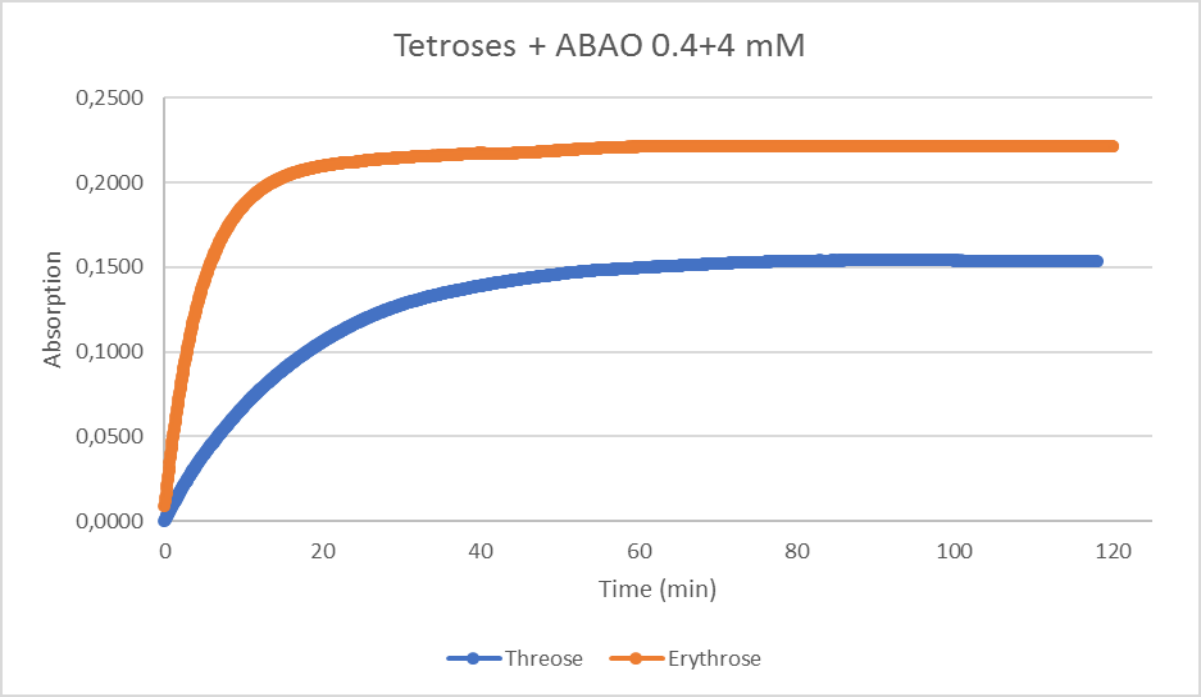

Figure 5: Lower concentration smoothens the curve of D-threose and D-erythrose.

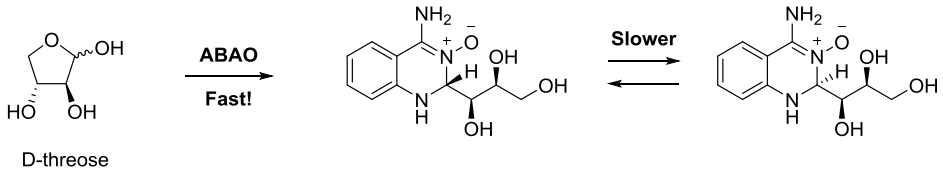

Scheme 13: Epimerization is significantly slower than adduct formation.

A hypothesis that was confirmed later by time resolved NMR is shown in **Scheme 13**. The hypothesis is that the adduct formation is a fast step, whereas the epimerization afterwards is a slower one. This explains the hump in the curve: one epimer has a higher absorption than the other epimer. After adduct formation is complete, one epimer overlays the other in the measurement until the epimer shift is finished. Time resolved NMR showed an epimer shift from 1:10 to 1:3 over time (**Figure 6**).

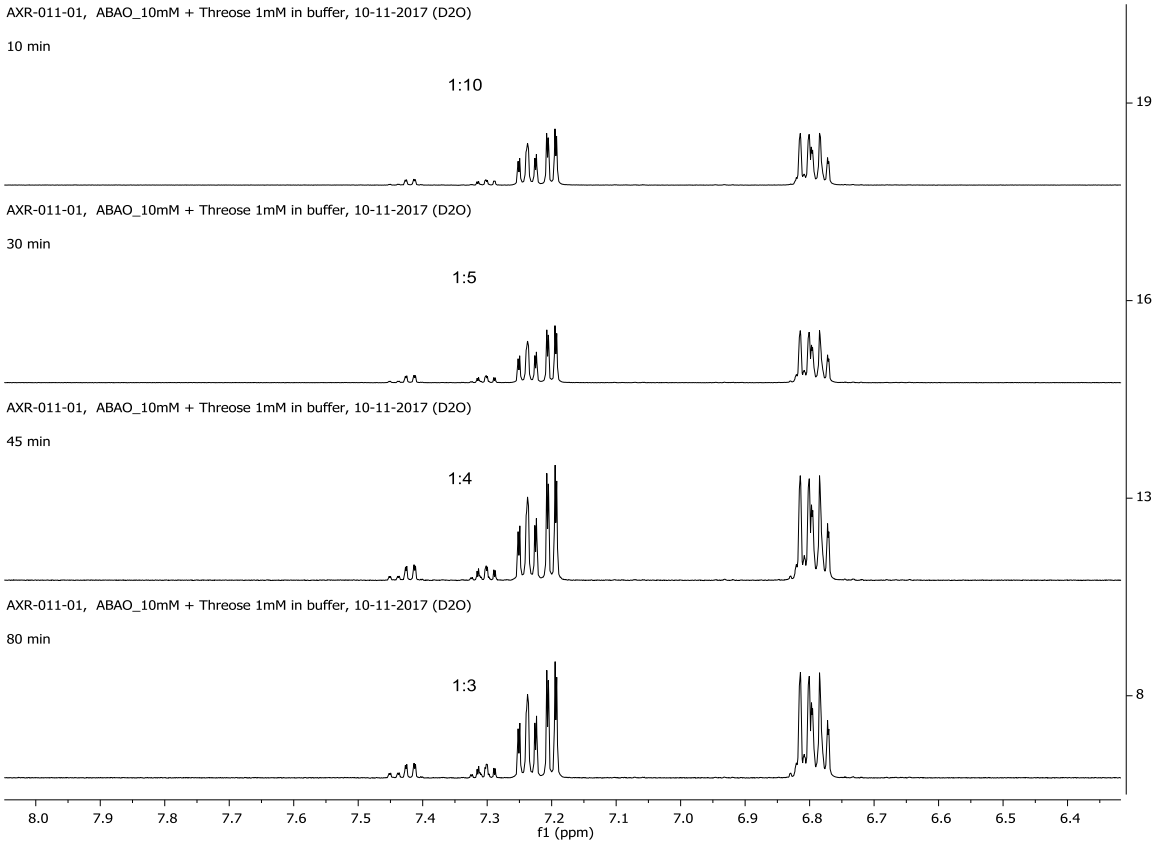

Figure 6: Time resolved epimer shift of D-threose.

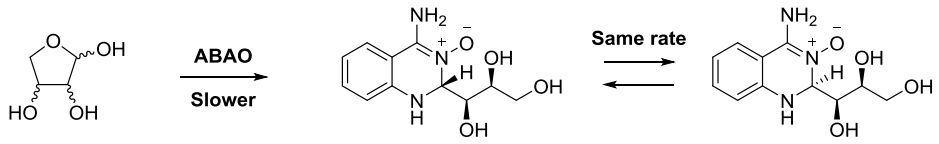

Scheme 14: Lower concentration slows down adduct formation.

As shown in **Scheme 14**, the lower concentration of the starting material slows down formation of the ABAO-adduct, which means the reaction rate of the adduct formation and the epimerization is more similar; therefore, the curve's hump is not visible anymore and a curve is obtained that can be used for determination of k_{app}.

To receive k_{app}, the calculation can be done by the software *Prism* or manually in *Excel*. With *Prism*, the corresponding time resolved curve of the measurement is analysed *via* the setting "one-phase association", which yields k_{app}.

If *Prism* is not available, the calculation can also be done in *Excel*. The logarithm is taken of the highest value of the curve and is subtracted with those data points to get a straight line. Finally, the trendline formula shows $k_{app.}$ It does not matter which method is used, as they yield both almost identical numbers (**Table 6**).

Table 6: Comparison of k_{app} between software and manual calculation.

Prism k_{app} ($s^{-1}*10^{-5}$)	Excel k_{app} ($s^{-1}*10^{-5}$)	Standard variation$*10^{-6}$
26.3	27.4	7.8
23.5	24.0	3.5
20.0	20.2	1.4
16.4	16.7	2.1

2.6 Introducing two sugar families

Table 7: Comparing the kinetic data of threose and erythrose.

Sugar	k_{app} ($s^{-1}*10^{-3}$)	Total k ($s^{-1}*10^{-3}$)
Threose	1.933	0.4833
Erythrose	3.075	0.7679

According to **Table 7** and also by visual comparison of the UV-curves it came apparent that, although their open chain content is similar, threose and erythrose have significantly different total K's. The phenomenon of different UV-curves is also visible with the pentoses and suggested that not only the aldose's open chain content influences reaction rate, but also the relative stereochemistry at the C2 and C3 positions next to the aldehyde carbon.

Instead of just assuming that product formation is equal for all aldoses as mentioned earlier in this thesis, it was decided to differentiate two families of sugars dependent on the O2/O3 diol being in *threo*- or *erythro*-configuration to determine correct numbers for the open chain content of aldoses. With these two families, the stereochemistry of other sugars can be taken into account (**Scheme 15**, **Scheme 16**); for example, the open chain content of arabinose (which is part of the *threo*-family (2,3-*threo*)) is calculated with the help of the threose k_{real}, whereas ribose, as member of the *erythro*-family (2,3-*erythro*) needs the erythrose k_{real}. It does not matter if a D- or L-aldose is used as they react identical.

To calculate the open chain content for an aldose (e.g. allose), the following equation is needed:

Open chain content = ((Total k_{allose}*_erythro_ k)/Total $k_{erythrose}$)*100

Erythro k is the correction factor (k_{real}), which is obtained if the open chain content (12% in the case of erythrose) is divided by the remaining forms (88%).

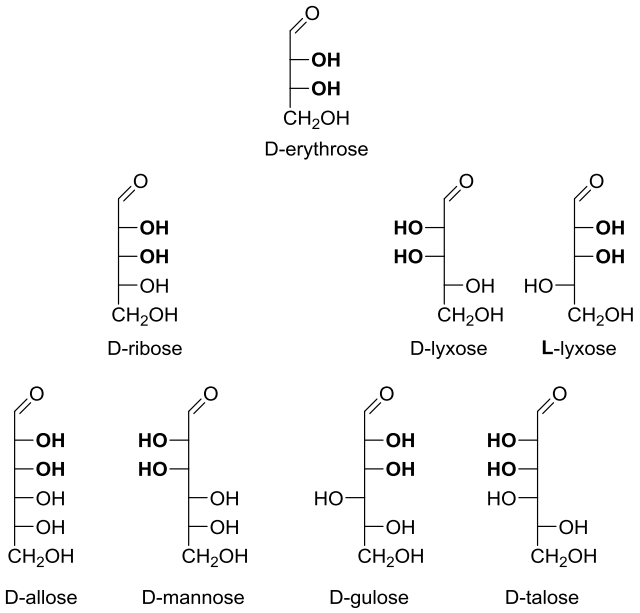

Scheme 15: 2,3-*erythro*-family of aldoses.

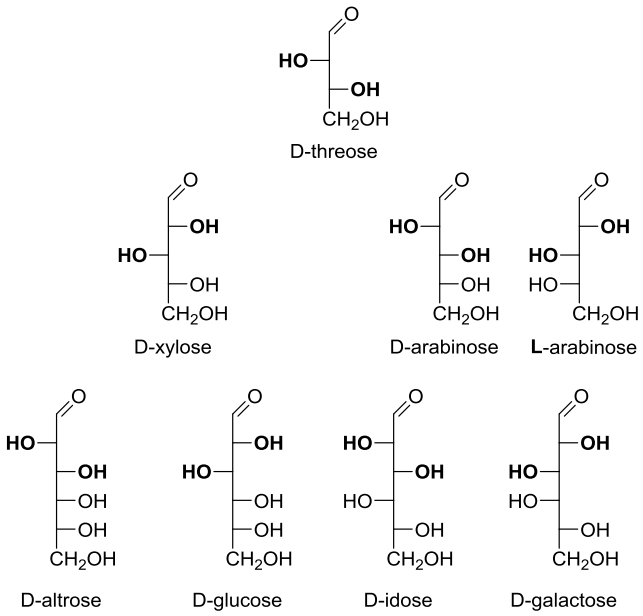

Scheme 16: 2,3-*threo*-family of aldoses.

2.7 Determination of the ratios of the tetrose anomers *via* NMR

To check if the commercially available tetroses are pure and moreover to determine their open chain content to be in accordance with the literature, D-threose and D-erythrose were analysed by NMR (600 Mhz, cryoprobe).

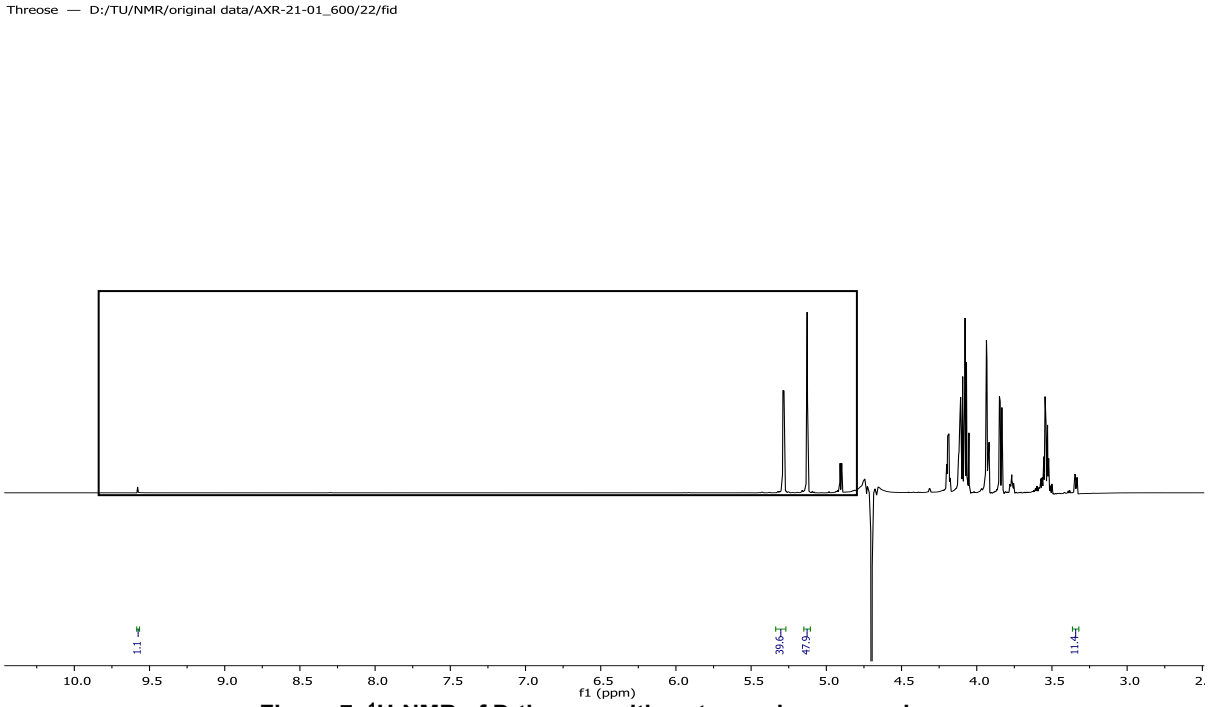

Figure 7: ^{1}H-NMR of D-threose with water peak suppression.

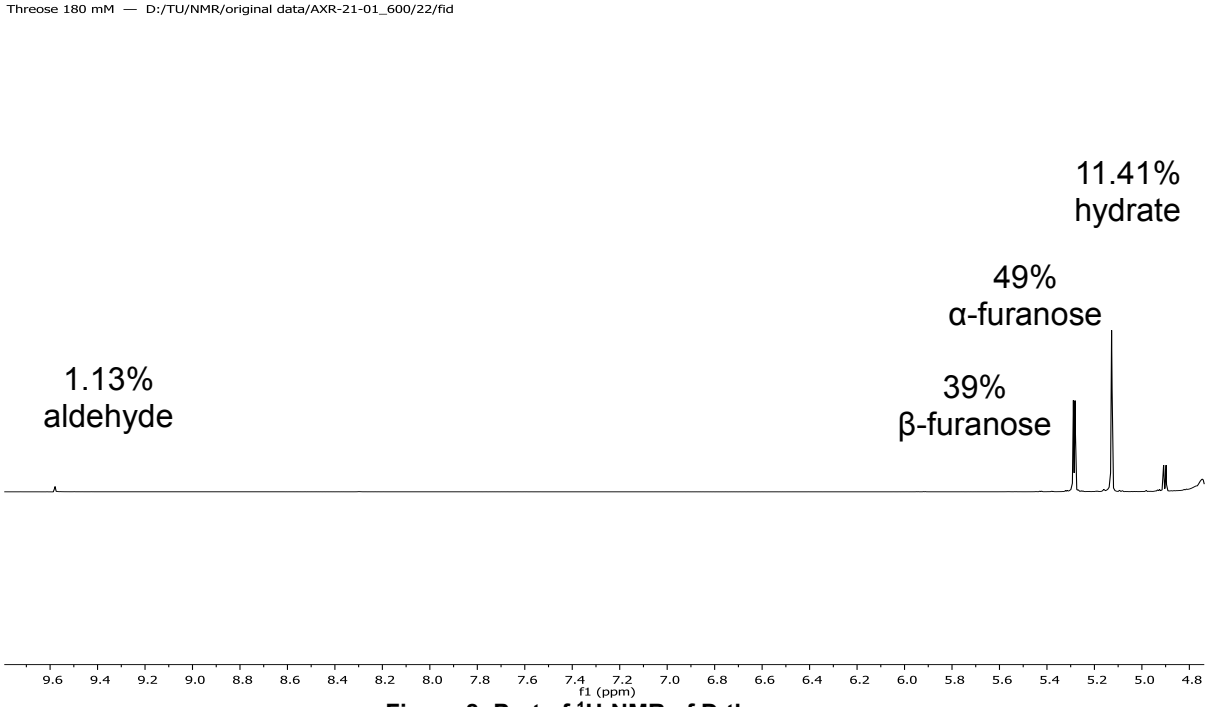

Figure 8: Part of ^{1}H-NMR of D-threose.

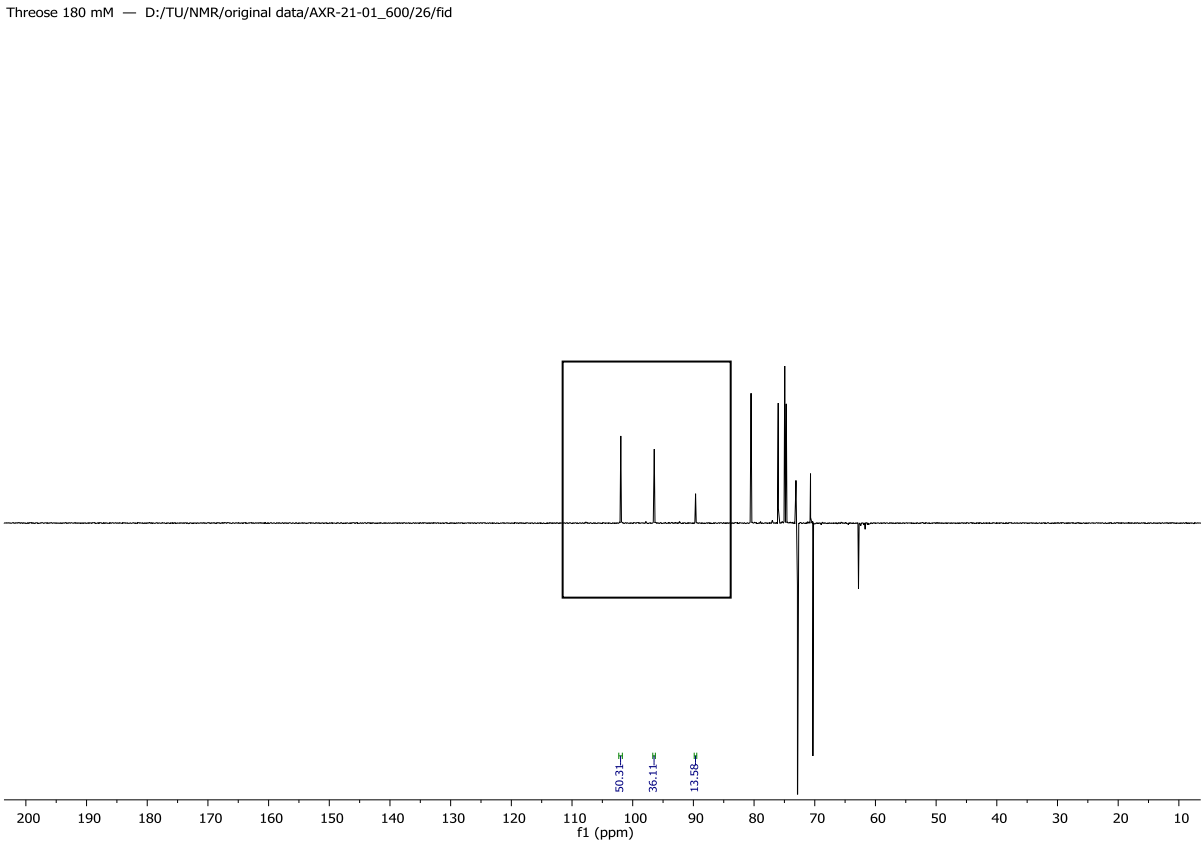

Figure 9: ^{13}C-APT-NMR of D-threose.

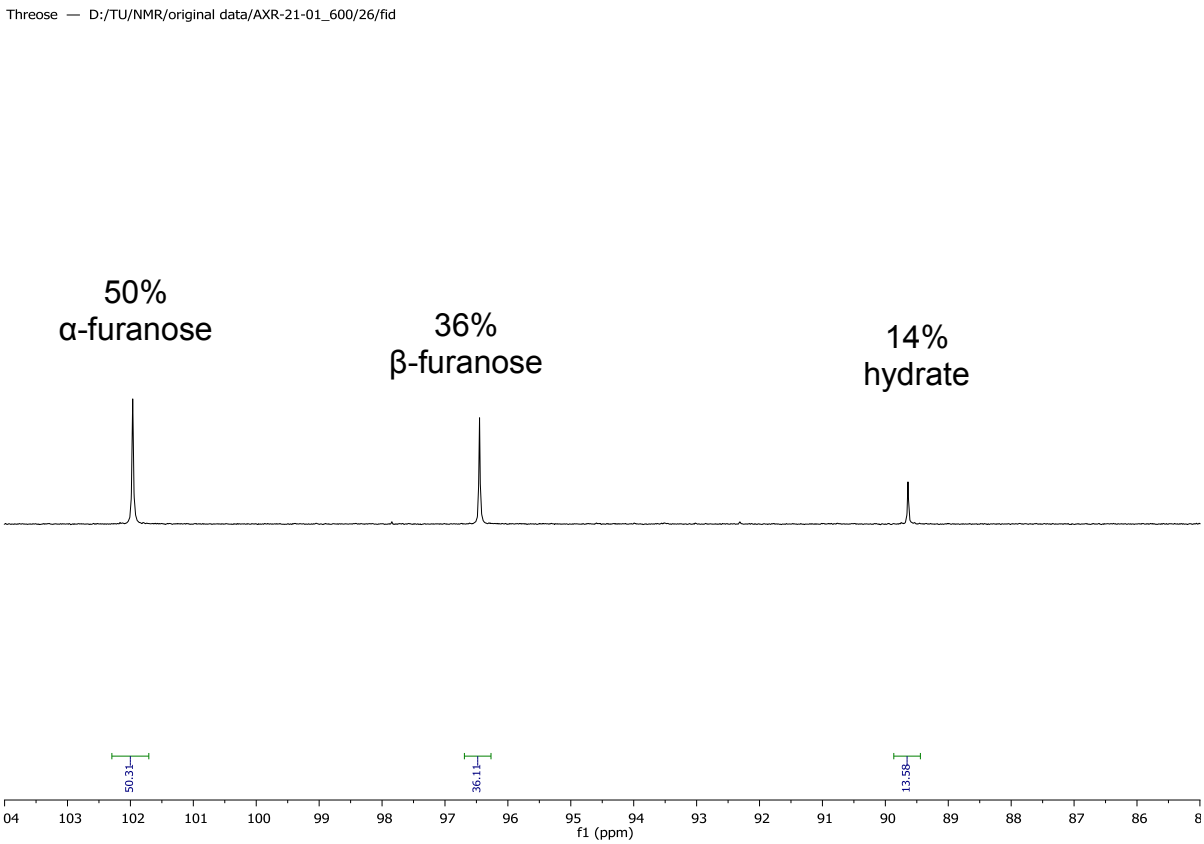

Figure 10: Part of ^{13}C-NMR of D-threose.

Commercially available threose is a syrup. Both ^{1}H-NMR (**Figure 7**) and ^{13}C-NMR (**Figure 9**) did not show any impurities and alpha, beta and open chain form had plausible ratios in consistence with the literature (48% α-furanose, 35% β-furanose, 1.2% hydrate and 1.2% aldehyde in ^{1}H-NMR, and 51.8% α-furanose, 37.6% β-furanose, 9.6% hydrate and 0.96% aldehyde in ^{13}C-NMR with $^{13}C_1$-enriched material)[8][14].

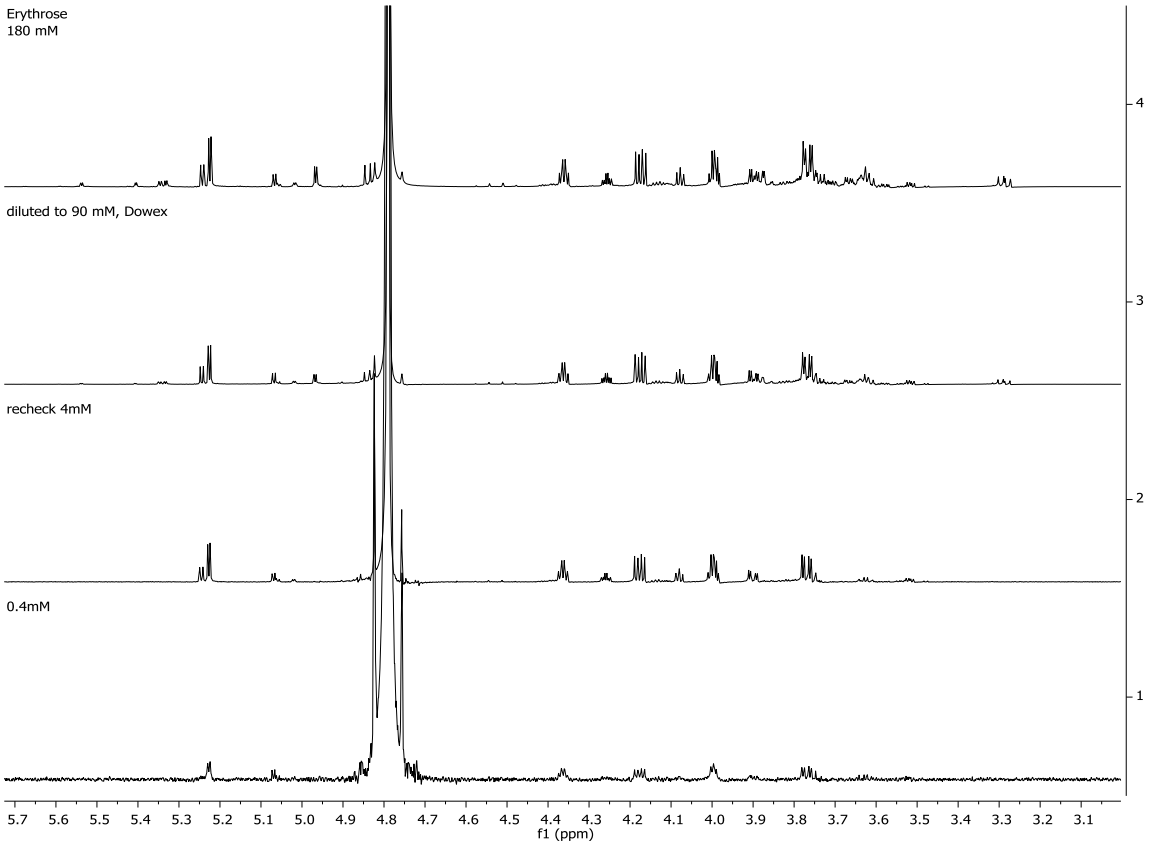

Figure 11: Part of ^{1}H-NMR of D-erythrose.

The ^{1}H-NMR of D-erythrose is shown in **Figure 11**, which is available as a 70% solution in water. A lot of putative dimer or oligomers were visible; a problem that has been already reported by Serianni et al. in 1979[13]. The concentration was lowered to 90 mM and the solutions were washed with Dowex, but there were still some dimers visible. Then the concentration was lowered again (4 mM). The NMR looked cleaner now, and hardly any putative dimers were observable, so this is clearly a concentration issue. More importantly, at the concentration that were best used for determination of tetrose kinetics (0.4 mM), the equilibrium should be entirely between monomeric species only, which could otherwise be considered responsible for the differences. However, with this concentration (0.4 mM) it was not

possible to determine the ratios as the noise of the baseline is too high. The composition of the 4 mM erythrose solution was 27.7% α-furanose, 60.7% β-furanose and 11.6% of hydrate, which is in good consistence with the literature[8]; whereas the aldehyde peak was not detectable.

2.8 Comparability of k's determined at different conditions

The plan was to translate k_{real} determined at necessary low concentration (0.4 mM) with e.g. threose to $k_{real's}$ determined at equally necessary high concentration of slow sugars.

To investigate if this approach is valid, a concentration screening with ribose and idose (substantially more open chain and thus faster than all other pentoses and hexoses) has been performed. Three types of series have been measured; in one series the concentration of the sugar is lowered at ABAO concentration of 40 mM (blue) (increasing sugar:ABAO ratio), in the second, the concentration of both starting reagents were lowered at equal ratio (green) and in the third series, ABAO concentration is lowered (purple). Additionally, a fourth series has been performed with idose where different sugar:ABAO ratios have been tested (red) (**Table 8**).

Table 8: Sugar & ABAO concentration screening to see if total k is different when concentration is changed.

Ribose (mM)	ABAO (mM)	k_{app} ($s^{-1}*10^{-5}$)	Total $k*10^{-3}$	Ratio
1	40	29.0	7.24	1:40
(4/3)	40	29.1	7.28	1:30
2	40	29.3	7.33	1:20
4	40	29.0	7.25	1:10
4	35	26.3	7.52	1:8.75
4	30	23.5	7.82	1:7.5
4	25	20.0	8.00	1:6.25
4	20	16.4	8.21	1:5
1	10	8.22	8.22	1:10
(4/3)	(40/3)	11.3	8.50	1:10
2	20	16.9	8.45	1:10

Idose (mM)	ABAO (mM)	K_{app} ($s^{-1}*10^{-5}$)	Total $k*10^{-3}$	Ratio
1	40	88.6	22.2	1:40
(4/3)	40	84.9	21.8	1:30
2	40	84.3	21.8	1:20
4	40	88.5	22.1	1:10
4	35	82.6	23.6	1:8.75
4	30	74.7	24.9	1:7.5
4	25	66.2	26.5	1:6.25
4	20	54.0	27.0	1:5
2	10	28.9	28.9	1:5
4	10	28.8	28.8	1:2.5
6	10	29.2	29.2	1:1.67
8	10	30.3	30.3	1:1.25
1	10	34.0	34.0	1:10
(4/3)	(40/3)	42.8	32.1	1:10
2	20	55.9	28.0	1:10

While it looked like that the total k of the 1:10 ratio series and the 1:20-1:40 ratio series are similar, this is not the case for the measurement of 4 and 40 mM for ribose and idose. Their total k's are similar to the 1:20-1:40 ratio series.

An interesting fact that could be observed is that the measurements which were performed with 40 mM of ABAO, regardless of the sugar concentration, is significantly different from the 1:10 series.

This variance of values is a phenomenon which is not fully explainable yet and needs further investigation.

Due to the fact that this screening has been performed with the plate reader, the variance could be explained with the instrument that is used as the wells are open and evaporation takes place as well as the temperature control which is not stable, and temperature slightly rises over time.

However, the current hypothesis is that if the reaction gets too fast, a different process becomes rate determining, or an accompanying process becomes less troublesome or gets overlaid (e.g. epimerization). Dependant on what consideration is right, one of the “k-families” yields right numbers.

2.9 Determination of kinetic of all pentoses and calculation of open chain content

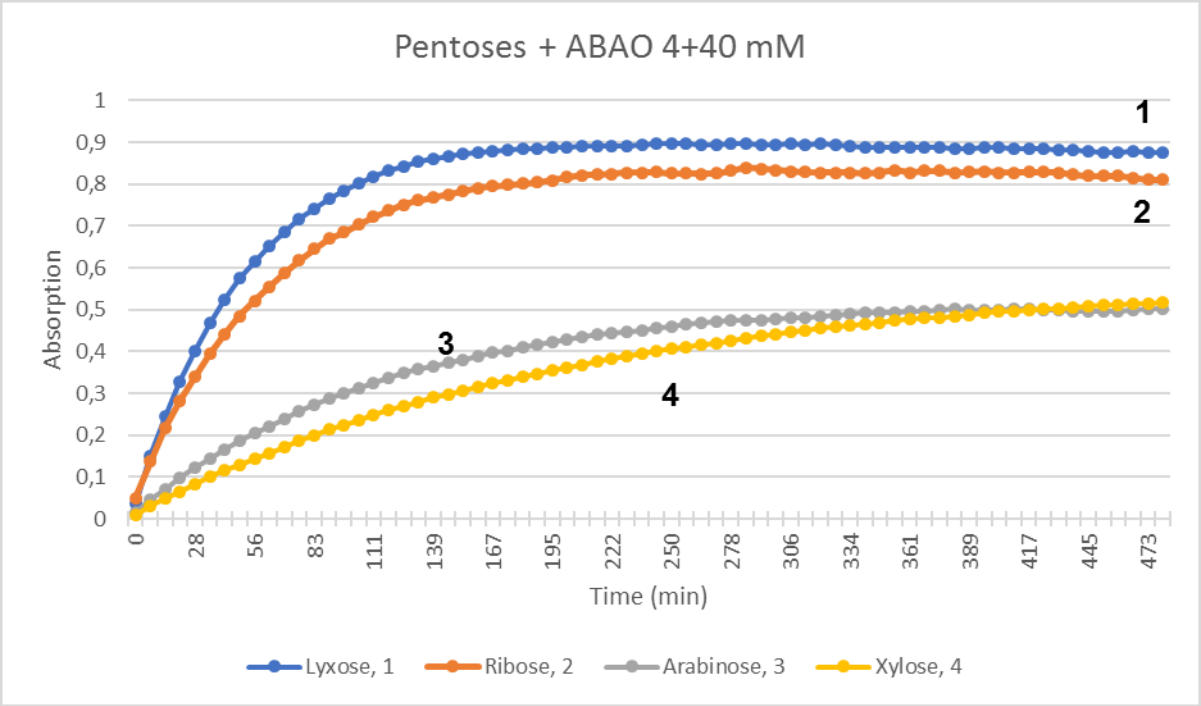

Figure 12: Pentoses reacting with ABAO.

As shown in **Figure 12**, according to their absorption there are clearly the 2 “sugar families” visible which were already mentioned earlier (*vide supra*): lyxose and ribose, having the same stereochemistry as erythrose, and arabinose and xylose are identical to threose in respect to the first three carbon atoms (**Scheme 17**).

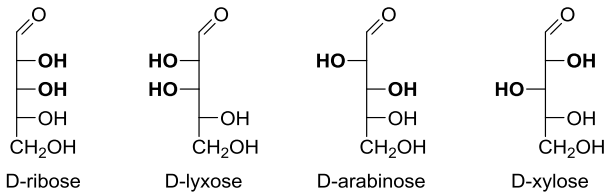

Scheme 17: Pentoses in the Fischer projection.

Table 9: Pentoses; their kinetic data reacting with ABAO and their calculated open chain content with *erythro*-/*threo*-correcting factor.

Sugar	k_{app} ($s^{-1}*10^{-3}$)	Total k ($s^{-1}*10^{-3}$)	Standard derivation of total $k*10^{-5}$	Open chain content (%)
Erythrose	3.075	768.8		
Threose	1.933	483.3		
Lyxose	0.35	8.80	9.4	0.16
Ribose	0.29	7.25	7.1	0.13
Arabinose	0.15	3.70	3.3	0.11
Xylose	0.082	2.04	5.4	0.06

2.10 Determination of kinetic of all hexoses and calculation of open chain content

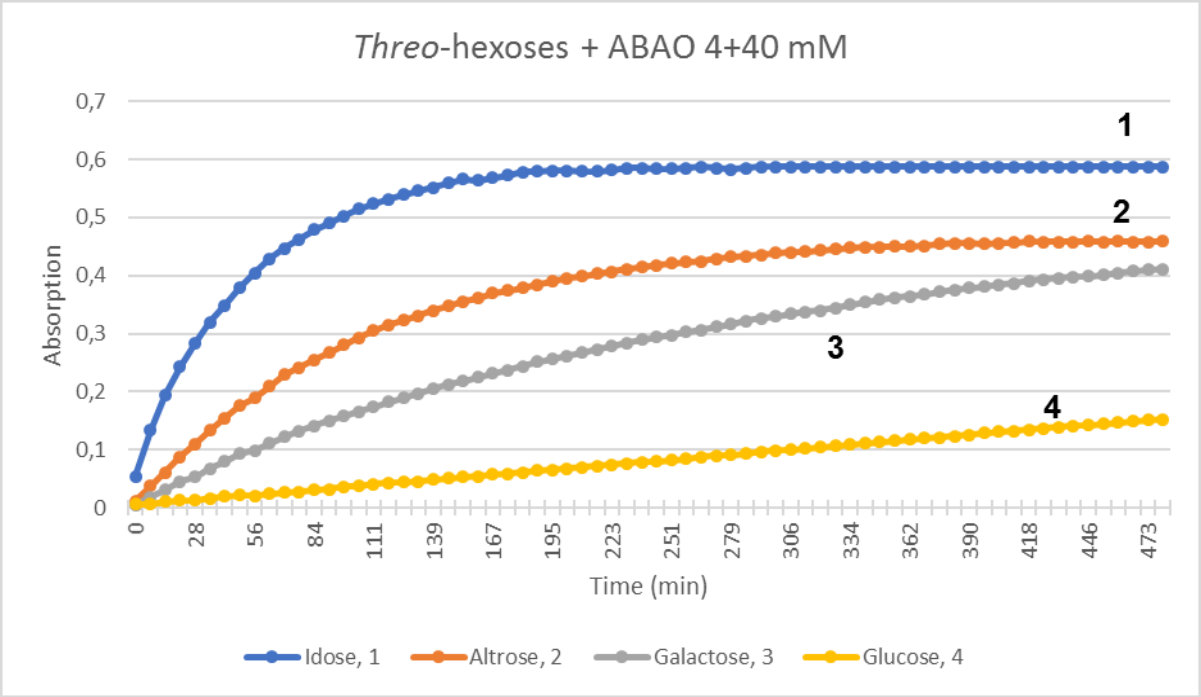

Figure 13: *Threo*-hexoses reacting with ABAO.

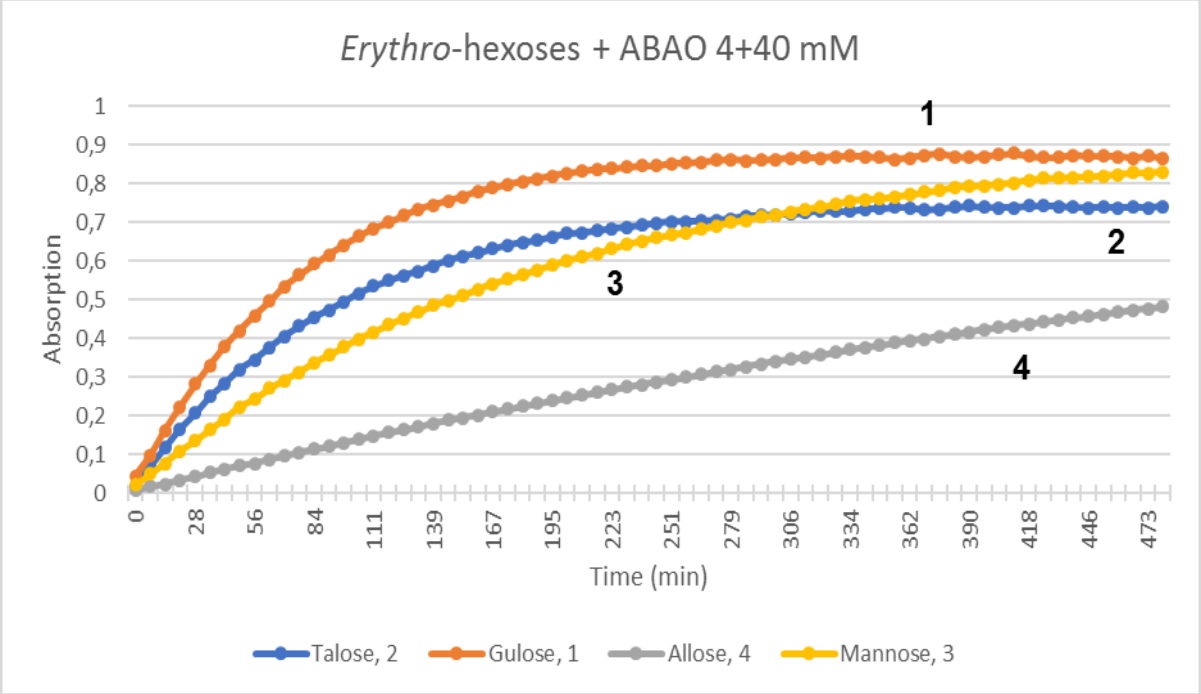

Figure 14: *Erythro*-hexoses reacting with ABAO.

Table 10: Hexoses; their kinetic data reacting with ABAO and their calculated open chain content with *erythro-*/*threo*-correcting factor.

Sugar	k_{app} ($s^{-1}*10^{-6}$)	Total k ($s^{-1}*10^{-4}$)	Standard derivation of total $k*10^{-8}$	Open chain content (%)
Erythrose	3075	7668		
Threose	1933	4833		
Altrose	150	44	250	0.11
Galactose	61	15	9.0	0.05
Allose	24	6		0.013
Glucose	9	2.2		0.007
Idose	885	221		0.66
Talose	180	46	150	0.08
Gulose	220	55	83	0.1
Mannose	89	22	228	0.04

The hexose kinetics are shown in **Figure 13** and **Figure 14** and **Table 10** shows the corresponding kinetic data. Within the hexoses, the “sugar families” are not so clearly visible as with the pentoses. Due to its very low open chain content published in the literature, the measurements of glucose and allose were performed over a longer period of time (48 hours for glucose and 24 hours for allose) in the photometer to get more reliable values for the open chain content because the product formation of those 2 sugars is so slow that their curves are still far away from their endpoint after 8 hours.

2.11 Open chain content – measured by kinetic method

Table 11: Aldoses and their open chain content measured by kinetic approach.

Erythro- family	Total k*10^{-4}	Open chain content (%)	Literature (%)
Erythrose	7688	12.0[a]	12-12.1[d]
Ribose	73	0.13	0.05-0.13[c]
Lyxose	88	0.16	0.03-0.1[c]
Allose	7	0.013	0.0085-0.011[b]
Talose	46	0.08	0.076-0.086[b]
Gulose	55	0.1	0.075-0.089[b]
Mannose	22	0.04	0.025-0.028[b]
Threo- family	**Total k*10^{-4}**	**Open chain content (%)**	**Literature (%)**
Threose	4833	12.5[a]	11-17[d]
Arabinose	37	0.11	0.03-0.1[c]
Xylose	20	0.060	0.002-0.07[c]
Idose	221	0.66	0.59-1[b]
Galactose	15	0.05	0.044-0.06[b]
Altrose	44	0.11	0.09-0.1[b]
Glucose	2.2	0.007	0.0089-0.011[b]

[a]determined *via* ^{1}H-NMR (see chapter 2.7)

[b]determined with $^{13}C_1$-labelled compounds by Zhu 2001[16]

[c]determined with $^{13}C_1$-labelled compounds by Drew 1998[15]

[d]determined *via* ^{1}H-NMR by Angyal 1980[14]

The measured open chain content by the kinetic approach and its content reported in the literature is shown in **Table 11**. Depending on which sugar is investigated, the kinetic method yields quite similar numbers, compared to numbers published in the literature that were determined by using $^{13}C_1$-labelled sugars (which is still the “gold standard” for measuring the open chain content of aldoses).

2.12 Preparative pentose adducts

It was still necessary to get reference material to be able to investigate phenomena such as the *syn*-/*anti*-epimerization and to check if ABAO-adducts can be synthesized in a preparative way. Therefore, D-lyxose and ABAO were dissolved in NH_4OAc and stirred overnight (**Scheme 18**)

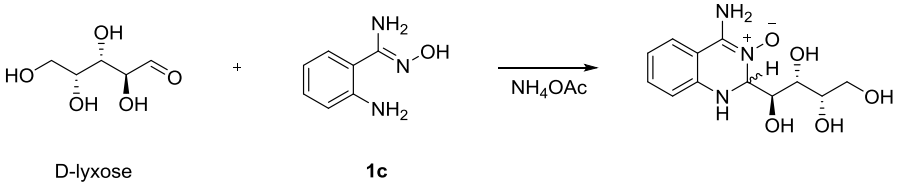

D-lyxose **1c**

Scheme 18: Synthesis of ABAO-adducts

After washing the solution with Et_2O and LP, the aqueous layer was lyophilised. NMR of the lyophilised product showed a diastereomer ratio of 80:20.

To isolate the more dominant diastereomer, some crystallisation experiments were made with mixtures of MeCN and H_2O. However, MeCN/H_2O 80:20 looked the most promising in NMR, so the product was purified *via* trituration with this mixture. (**Scheme 19**).

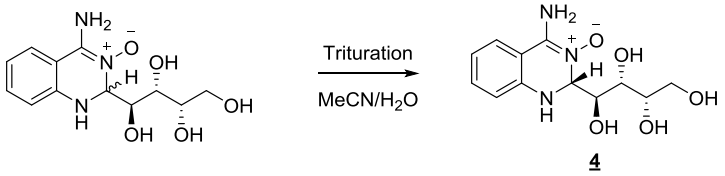

4

Scheme 19: Purification of ABAO-adducts.

The brown, sticky syrup turned into a colourless solid; but the crystals formed were too small to be measured to get a crystal structure. In the mother liquid, however, the crystals that were formed after a few weeks were big enough to be measured by X-ray crystallography with a Bruker D8 Venture diffractometer system equipped with Cu micro source and Photon II detector (**Figure 15**).

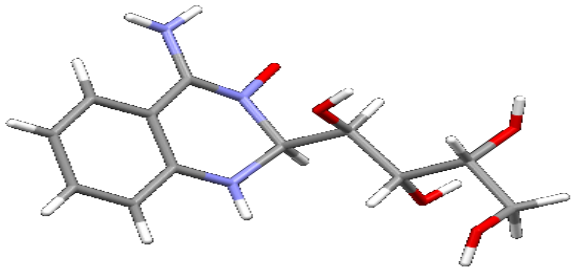

Figure 15: Crystal structure of *anti-syn*-epimer.

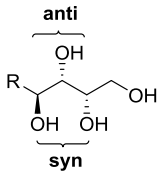

Figure 16: Isolated epimer in *anti-syn*-configuration.

The more dominant isomer that was isolated is the *anti-syn*-epimer (**Figure 16**). The name of this structure is, according to IUPAC (R)-4-amino-2-((1S,2S,3S)-1,2,3,4-tetrahydroxybutyl)-1,2-dihydroquinazoline 3-oxide.

In the time resolved NMR, epimerization of the pure epimer could be observed as 2 epimers were visible again. The epimer shift changed from 90:10 to 80:20 and was completed after 2,5 hours. Interestingly, the product with its epimer ratio looked identical in NMR when it was measured again 2 days later.

To make sure that this procedure is also applicable to other aldoses, the procedure shown in **Scheme 18** repeated with the remaining pentoses ribose, arabinose and xylose. Crude NMR showed full conversion of the starting material, however, it was not possible to isolate the major epimer after lyophilisation as mentioned in **Scheme 19**. Instead of one phase, there was a MeCN-phase and a water phase. MeOH was added to get a single-phase solution and it was stored in the fridge overnight. The next day, a white solid precipitated in the vial that contained ribose. The crystalline material was dried in *vacuo*; NMR showed a diastereomeric ratio of 3:1, so more of the minor epimer was present.

Interestingly, this experiment was only successful once in a small scale and only with ribose, and it was not possible to isolate the other major epimers.

2.13 Applications

2.13.1 Ribose versus 2-deoxy-ribose

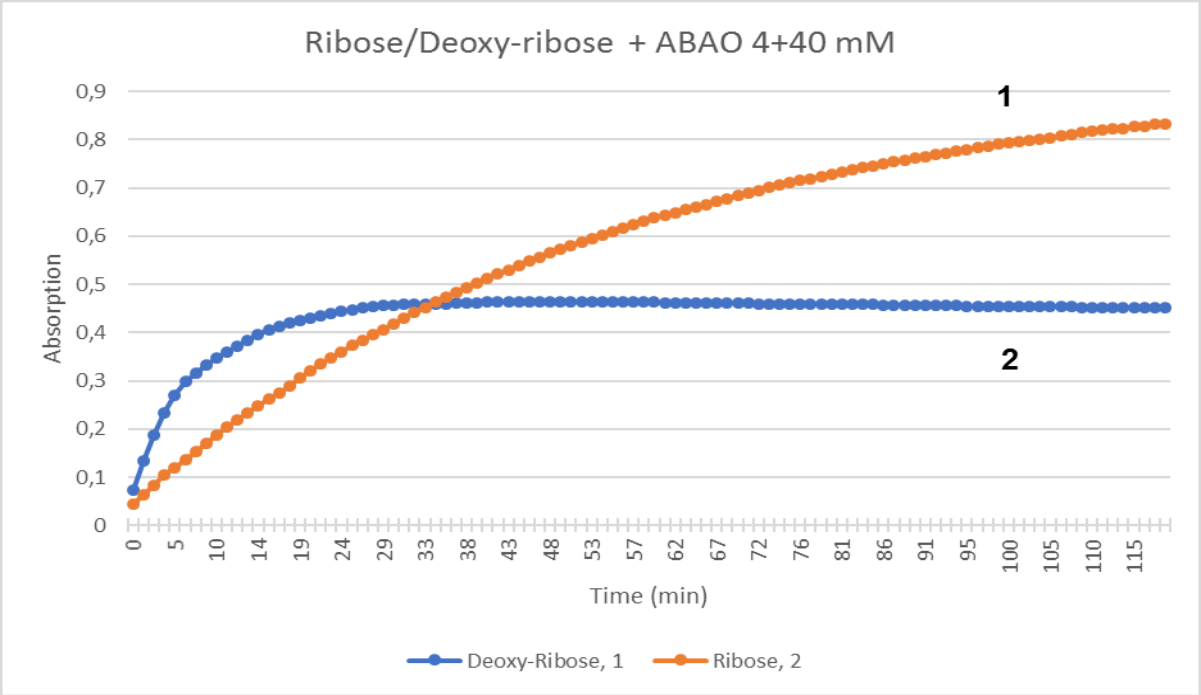

Figure 17: 2-deoxy-ribose versus ribose.

Due to the fact that *erythro*- and *threo*- sugars had to be separated to yield correct numbers, the behaviour of 2-deoxy-ribose with ABAO was not quite surprising. As shown in **Figure 17**, it is important to emphasize that standard aldoses cannot simply be compared with deoxy-aldoses. 2-Deoxy-D-ribose has no oxygen atom in position 2 (**Scheme 20**) and as mentioned before, the adduct formation not only depends on how high the aldehyde content is, but also on the chemical moieties on C2 and C3. Although the open chain content of 2-Deoxyribose (0.18%)[9] is not significantly higher than ribose, due to the inductive effect of the hydrogen vs. the hydroxy group, 2-Deoxy-D-ribose is significantly faster than D-ribose[9].

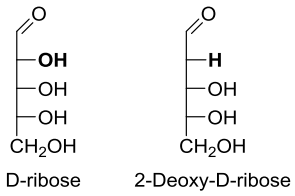

Scheme 20: D-ribose and 2-Deoxy-D-ribose in the Fischer projection.

2.13.2 Benzyl-sugars

Aldoses with a benzyl protecting group – 2-O-benzyl-pentoses and 3-O-benzyl-hexoses are used within the research group in a different project where the aldehyde-group of the sugar is addressed as well. To get a better understanding of the reaction behaviour of benzyl-sugars, reactions with ABAO were performed for comparison.

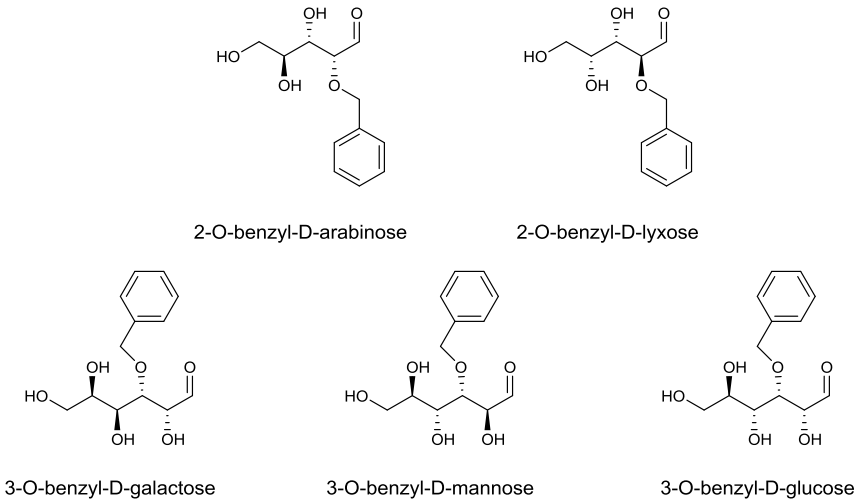

Figure 18: Benzyl-sugars used in this measurement.

The benzyl-sugars that are used in this measurement are shown in **Figure 18**. The benzyl-pentoses have the protecting group at the C2-carbon, whereas the benzyl-hexoses are substituted with the benzyl-group at C3. A benzyl-group at the C2-carbon means the aldehyde carbon cannot get attacked so easily anymore. This would lead to lower reaction rates, compared to the unsubstituted pentoses.

A benzyl-group at C3 would either influence the open chain content or does not influence the reaction rate significantly.

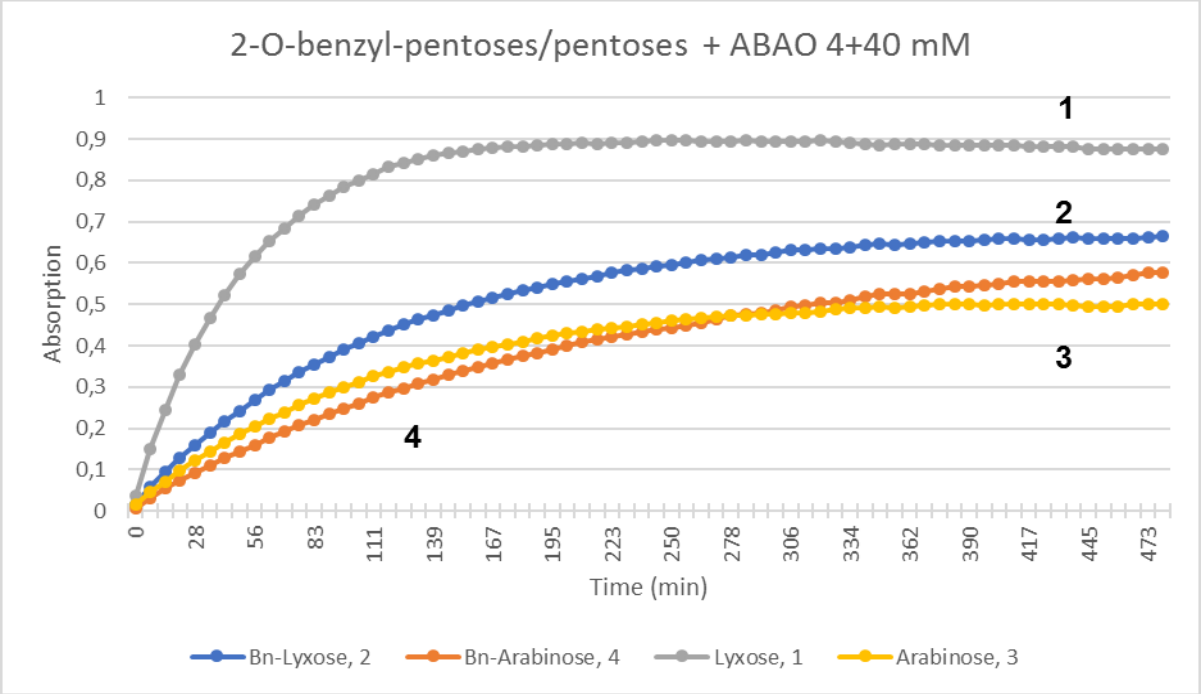

Figure 19: 2-O-benzyl-pentoses and pentoses reacting with ABAO.

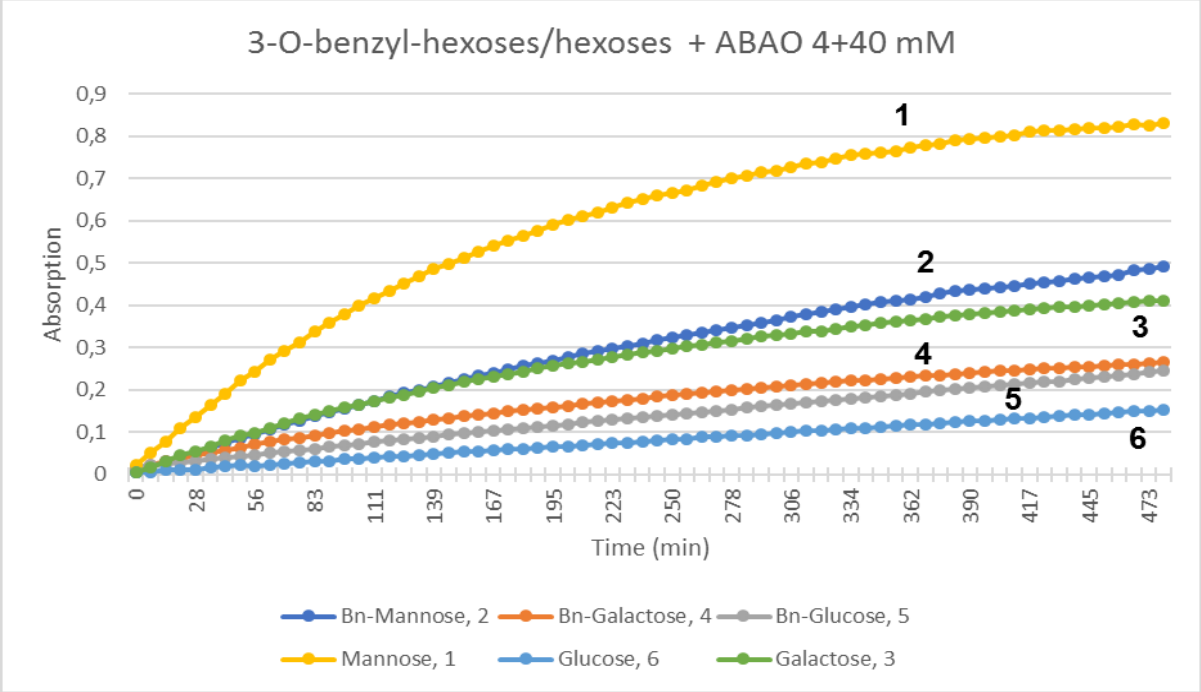

Figure 20: 3-O-benzyl-hexoses and hexoses reacting with ABAO.

As shown in **Figure 19**, the 2-O-benzyl-pentoses reacted as expected. The benzyl-group in position 2 leads to lower product formation than the corresponding non-protected sugar.

Interestingly, 3-benzyl-hexoses did not react as expected. The reaction rate of benzyl-galactose is similar to regular galactose and benzyl-mannose reacts only half as fast as mannose (**Table 12**).

However, benzyl-glucose is 10 times faster than glucose. A possible explanation could be that the benzyl-group destabilizes the dominant form of glucose, the pyranose form and therefore, more open chain form is available.

Table 12: Comparing kinetic data of pentoses/hexoses and their corresponding benzyl-derivatives.

Sugar	k_{app} ($s^{-1}*10^{-5}$)	Total $k*10^{-4}$
Lyxose	35	88
Benzyl-lyxose	14	35
Arabinose	15	37
Bn-arabinose	8	20
Mannose	9	22
Bn-mannose	4	10
Galactose	6	15
Bn-galactose	5	12
Glucose (8 hrs)	0.09	0.2
Bn-glucose	0.78	2

Unfortunately, at this point it is not possible to calculate their open chain content because there is no reference sugar – benzyl-threose or -erythrose – easily available with an open chain content high enough to be measured *via* NMR.

2.13.3 Determination of open chain content of 2,3-O-isopropylidene erythrose- the real case

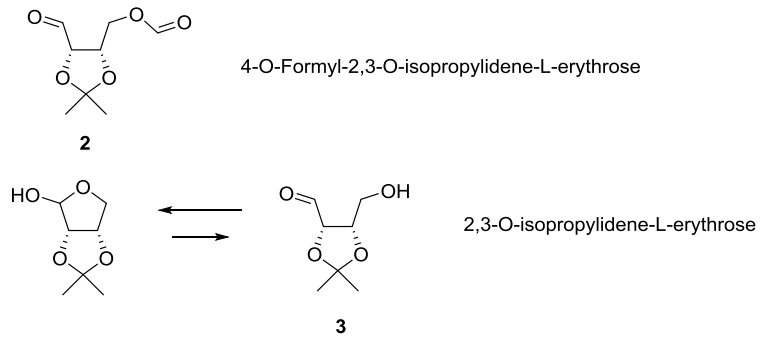

Scheme 21: Protected erythrose (2) is only available as aldehyde, 3 can form a lactol.

4-O-Formyl-2,3-O-isopropylidene-L-erythrose (**2**) and 2,3-O-isopropylidene-L-erythrose (**3**) were used by the research group in an earlier project[17]. In this publication, a study about Indium- and Zinc-mediated acyloxyallylation of protected and unprotected aldotetroses was conducted. However, it was not possible to yield any product with **3** because it is able to form a very stable lactol form (**Scheme 21**), and therefore, it is hardly available as an aldehyde. Formyl-isopropylidene-erythrose (**2**) cannot form any other configurations and is only available as an aldehyde, but it is unstable. For the project by Draskovits et al, high product formation was wanted with using the isopropylidene-erythrose (**3**) due to its high stability and its more convenient synthesis than **2**.

Although it is not possible yet to calculate the open chain content of protected sugars whose reference sugar's open chain content is not known, sugar derivatives are an interesting field where this method can predict the reactivity of the aldehyde group. 4-O-Formyl-2,3-O-isopropylidene-L-erythrose and 2,3-O-isopropylidene-L-erythrose are both derivatives from erythrose, whose open chain content has already been discussed earlier in this thesis.

4-O-Formyl-2,3-O-isopropylidene-L-erythrose is not stable and had to be prepared right before the kinetic measurement.

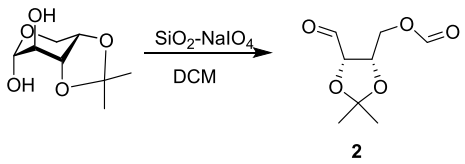

Scheme 22: Synthesis of 4-O-Formyl-2,3-O-isopropylidene-L-erythrose.

As shown in **Scheme 22**, the starting material, arabinose-acetonide, was taken up in dry DCM and SiO_2-$NaIO_4$ was added. After complete conversion, the reaction mixture was filtered, and the silica gel was washed with $CHCl_3$.

This protected erythrose cannot cyclise by itself to form a cyclic form; therefore, it is only available as an aldehyde. 2,3-O-isopropylidene-L-erythrose in contrast can close to form a lactol, which does not react with ABAO and is the dominant form of this derivative, but it is also in equilibrium with the aldehyde form, although again at levels that cannot be quantified by standard techniques (**Scheme 21**).

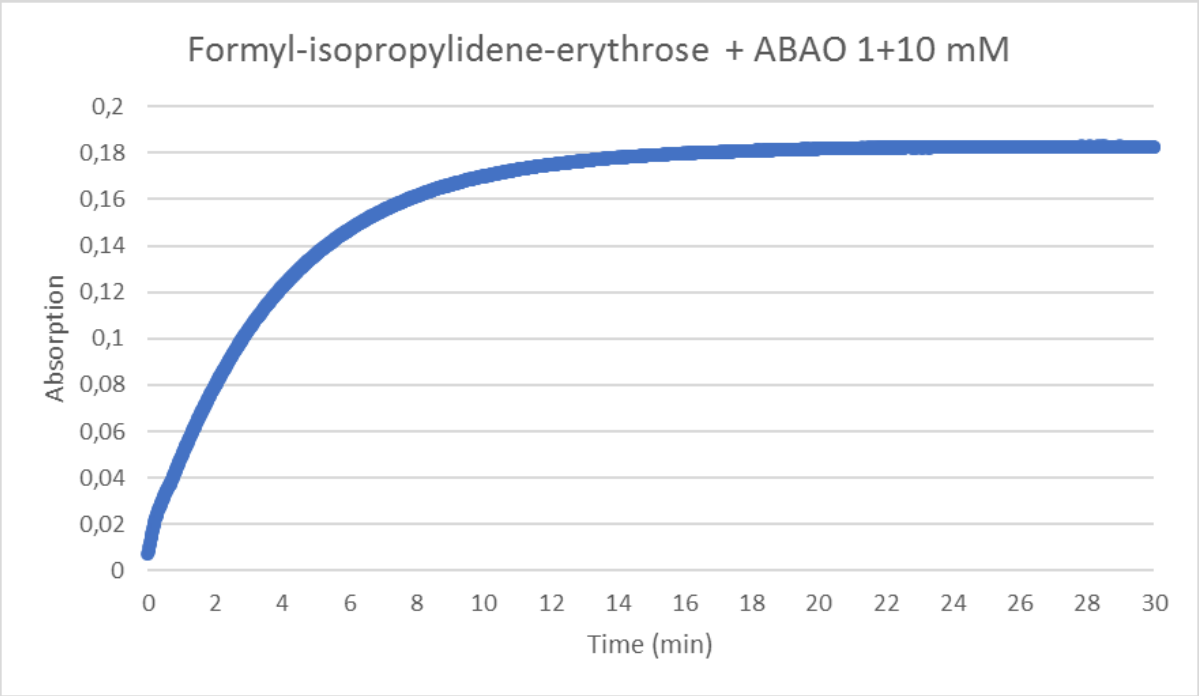

Figure 21: 4-O-Formyl-2,3-O-isopropylidene-L-erythrose reacting with ABAO.

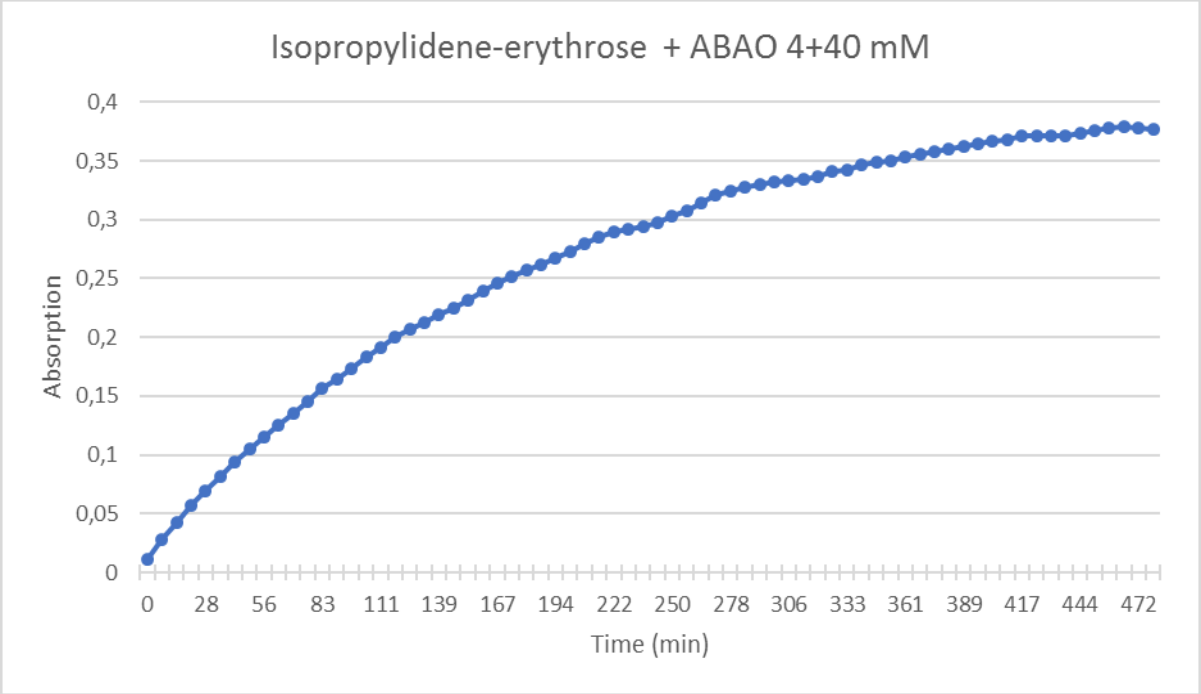

Figure 22: 2,3-O-isopropylidene-L-erythrose reacting with ABAO.

Table 13: Erythrose derivatives - their kinetic data and open chain content.

Sugar	k_{app} (s^{-1} *10^{-5})	Total K*10^{-3}	Open chain content (%)
Erythrose	307	769	12
2	435	435	100
3	8.7	2.2	0.5

Figure 21, **Figure 22** and **Table 13** show the kinetic data of the said sugar derivatives. The open chain content of erythrose was discussed already earlier in this thesis and it can be assumed that 4-O-Formyl-2,3-O-isopropylidene-L-erythrose has an open chain content of 100%, as it cannot form any other configurations. Therefore, the open chain content of 2,3-O-isopropylidene-L-erythrose can be calculated *via* the total k of the 2 sugar derivatives, which is 0.5%.

Although 4-O-Formyl-2,3-O-isopropylidene-L-erythrose is only available as an aldehyde, the adduct formation compared to erythrose is significantly slower. A possible explanation could be that the amino-group of the ABAO cannot attack the aldehyde group so easily anymore because of the steric bulk of the ester moiety.

2.14 Conclusion

The aim of this thesis was to introduce a new method to measure the open chain content of reducing sugars. In the past, mostly NMR was used which takes at least several days to get exact values.

Via adduct formation between 2-amino-benzamidoxime derivatives and aldoses, it is possible to calculate the open chain content of reducing sugars. Usually, a maximum of 8 hours is needed to receive a curve and to estimate the reactivity of the aldehyde group or to measure the open chain content of a sugar sample. This is a big step forward, as this method yields quite similar numbers compared to numbers published in the literature that were measured by NMR (by using $^{13}C_1$-enriched material), which is still the “gold standard” for measuring the open chain content of aldoses.

Furthermore, it is a cheap and simple method and only a photometer or a plate reader is needed. ABAO is purchasable so no synthesis in advance is needed, the buffer can be done quickly and after pipetting ABAO and the sample together, the measurement can already be started.

On the other side, regarding the open chain content, it is highly dependable on the reference sugars, whose open chain content were determined by NMR. To get exact data, time consuming multiple measurements *via* NMR and photometer are needed. It was not possible to separate the two k’s within this project, which was the reason why the “sugar families” were introduced. There are also still phenomena which are not fully explainable yet and need further investigation.

However, this method yields quite exact values for the open chain content of aldoses compared to numbers published in the literature, and it can be also be used for a better understanding of the reactivity of unknown or little-known structures.

2.15 Abstract

If an aldose is dissolved in water in its crystalline state, an equilibrium of different forms of the dissolved sugar is observed after a certain amount of time: α- and β-pyranoses and -furanoses and the open chain forms, hydrate and aldehyde-form. The proportion of the cyclic forms is higher than the open chain forms at equilibrium; the hydrate and aldehyde are only available in low to medium concentrations (<0.1% in most hexoses, 12% in tetroses).

In the past, various methods have been used to measure the open chain content of aldoses. However, either the method was not suitable for it (e.g. polarimetry) or it is a time consuming and expensive one (e.g. NMR with $^{13}C_1$-enriched material).

In this diploma thesis, a kinetic model was set up to measure the open chain content of reducing sugars (**Scheme 23**).

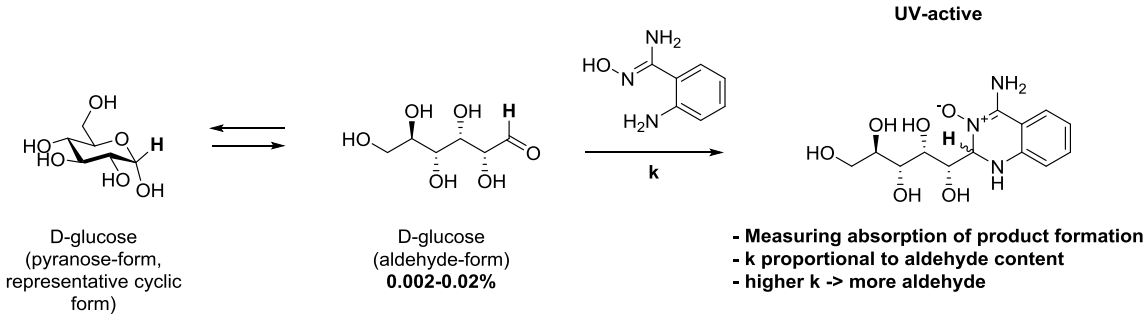

Scheme 23: Kinetic model to measure the open chain content of aldoses.

Therefore, different 2-aminobenzamidoximes have been synthesized and the reaction conditions were optimized to this system. It was found that not only the aldehyde content of the sugar influences the kinetics, but also the stereochemistry. To yield exact values, a differentiation between 2,3-*threo* and 2,3-*erythro* was necessary (**Scheme 24**).

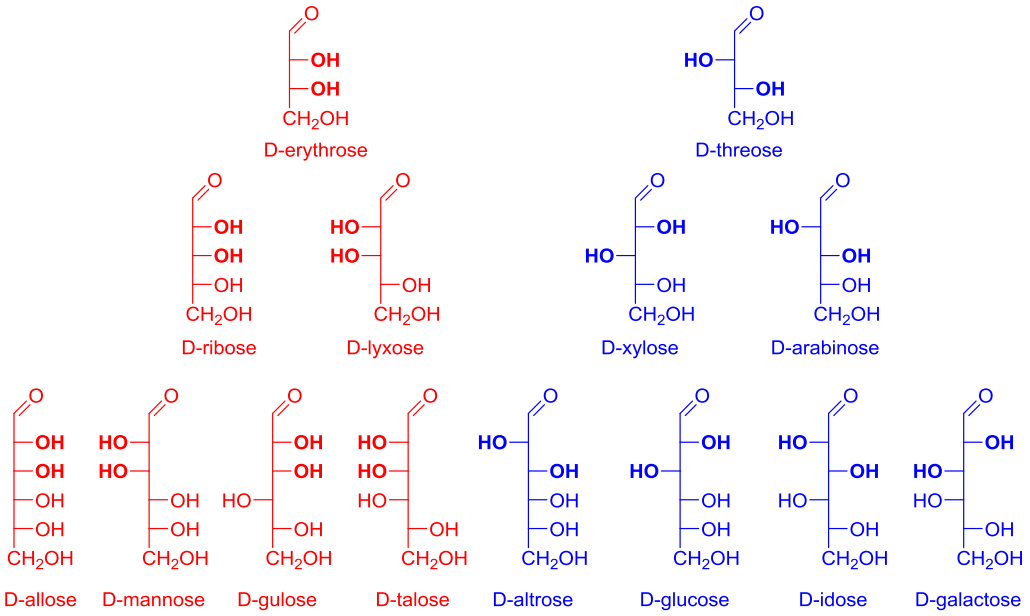

Scheme 24: 2,3-*erythro*-sugars (red) and 2,3-*threo*-sugars (blue).

In summary, this model, which is easy to handle and requires little equipment yields exact values for the open chain content of reducing sugars. This is useful for reactions where only the aldehyde-form of the sugar is reacting to estimate reactivity and yield.

2.16 Deutsche Kurzfassung

Wenn eine Aldose in kristalliner Form in Wasser gelöst wird, stellt sich nach einiger Zeit ein Gleichgewicht von verschiedenen Formen ein: α- und β-Pyranosen und -Furanosen, sowie die offenkettigen Formen, Hydrat und Aldehyd-Form. Das Gleichgewicht liegt dabei auf Seite der cyclischen Formen, Aldehyd und Hydrat liegt nur in sehr geringer bis mittlerer Konzentration (<0,1% bei den meisten Hexosen, 12% bei den Tetrosen) vor.

Früher wurde bereits versucht den offenkettigen Anteil von Aldosen exakt zu messen. Entweder eignete sich die Methode dafür nicht (wie z.B. Polarimetrie) oder diese ist sehr zeitaufwendig und teuer (z.B. NMR mit $^{13}C_1$-angereichertem Material).

In dieser Diplomarbeit wurde ein kinetisches Modell aufgestellt, um den offenkettigen Anteil von reduzierenden Zuckern zu berechnen (**Abbildung 1**).

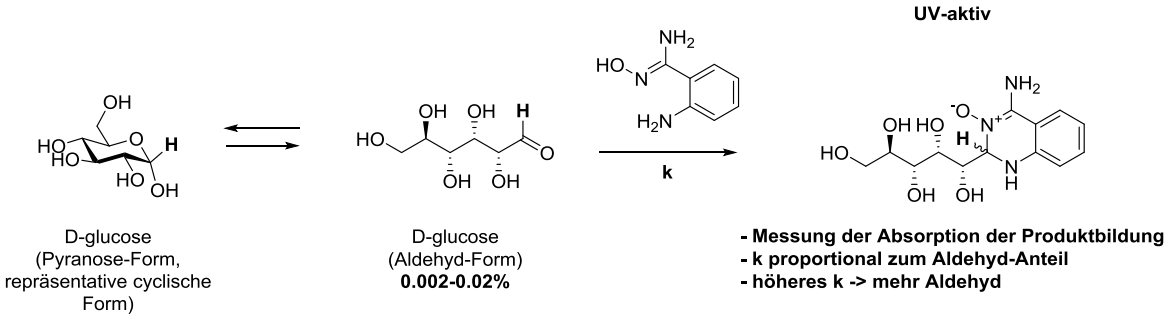

Abbildung 1: Kinetisches Modell zur Berechnung des offenkettigen Anteils von Aldosen.

Hierzu wurden verschiedene 2-Aminobenzamidoxim-Derivate synthetisiert und die Reaktionsbedingungen an dieses Modell angepasst und optimiert. Es stellte sich dabei heraus, dass nicht nur der Aldehyd-Anteil bei der Kinetik eine Rolle spielt, sondern auch die Stereochemie: Um genaue Werte zu erhalten, war eine Unterscheidung zwischen 2,3-*threo* und 2,3-*erythro* nötig (**Abbildung 2**).

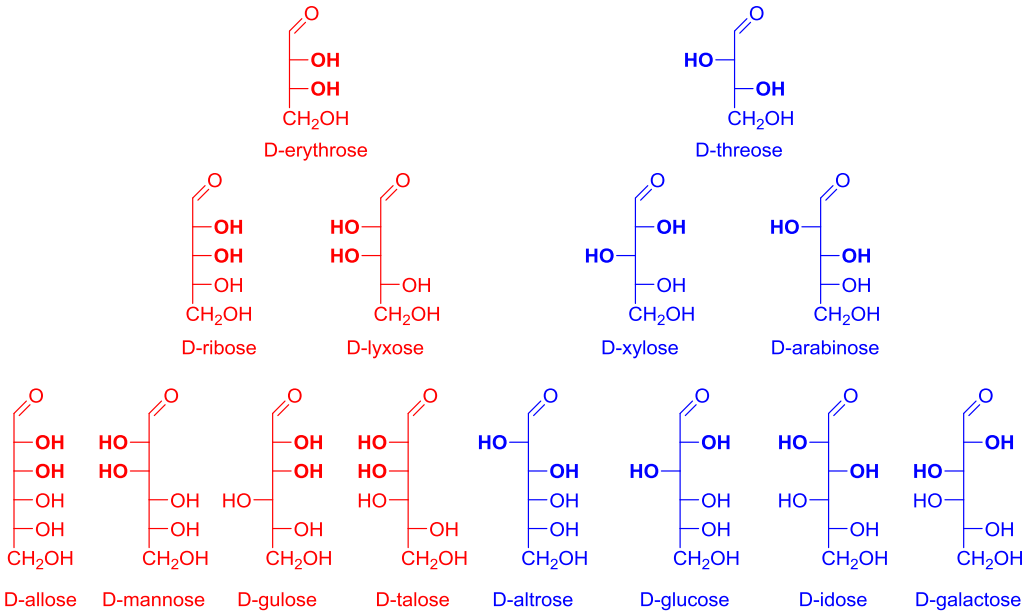

Abbildung 2: 2,3-*erythro*-Zucker (rot) and 2,3-*threo*-Zucker (blau).

Zusammenfassend bleibt zu sagen, dass dieses Modell schnell, einfach und mit wenig Equipment relativ genaue Werte für den offenkettigen Anteil von reduzierenden Zuckern erzeugt. Damit lässt sich bei Reaktionen, in denen nur die Aldehyd-Form des Zuckers reagiert, eine Abschätzung bezüglich der Reaktivität und der Ausbeute treffen.

3 Experimental part

3.1 General notes

Chemicals

Chemicals were purchased from chemical suppliers.

Chromatography

TLC was performed on aluminium coated silica gel 60 F_{254}. The spots were visualized with UV-light or anisaldehyde solution (180 ml EtOH, 10 ml anisaldehyde, 10 ml H_2SO_4 conc., 2 ml acetic acid).

Melting point

Melting points were determined by a Leica Galen III Kofler.

HR-MS

HR-MS analysis was carried out from water solutions (concentration: 10 µM) by using an HTC PAL system autosampler (CTC Analytics AG, Zwingen, Switzerland), an Agilent 1100/1200 HPLC with binary pumps, degasser and column thermostat (Agilent Technologies, Waldbronn, Germany) and Agilent 6230 AJS ESI–TOF mass spectrometer (Agilent Technologies, Palo Alto, United States).

NMR spectroscopy

^{1}H-NMR and ^{13}C-NMR spectra were recorded from D_2O or DMSO-d_6 solutions on a Bruker Avance UltraShield 400 (400 MHz) and 600 (600 Mhz, cryoprobe) spectrometer. Chemical shifts are reported in ppm relative to the nominal residual solvent signal of the solvents.[18]

D_2O (^{1}H: 4.79 ppm)

DMSO-d_6 (^{1}H: 2.50 ppm, ^{13}C: 39.52 ppm)

Example of numbering change from ABAO to ABAO-adduct

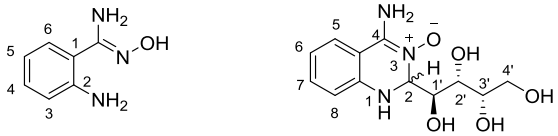

3.2 Standard procedures

3.2.1 Standard procedure (SP1) for the preparation of 2-Aminobenzamidoxime derivatives (1b, 1c)

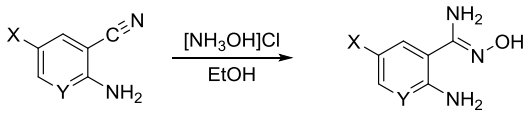

(**X**=H, **Y**=N), **Ib**
(**X**=H, **Y**=C), **Ic**

(**X**=H, **Y**=N), **1b**
(**X**=H, **Y**=C), **1c**

2-Aminobenzamidoximes were prepared according to the literature.[11]

The corresponding aminonitrile **I** (12 mmol) was dissolved in EtOH (24 ml) and hydroxylamine hydrochloride (19 mmol) was added. To dissolve the hydroxylamine completely, water (8 ml) was added, then $NaHCO_3$ (23 mmol) was added and the solution was stirred 5 min at room temperature. Although $NaHCO_3$ did not get dissolved completely, the solution was refluxed overnight. The reaction was monitored *via* TLC (LP/EtOAc 1:1). The next day, TLC indicated that there was no starting material left and the reaction was complete.

The mixture was concentrated and neutralized with 2N HCl. The aqueous solution was extracted with EtOAc. TLC showed that the first washing step contained some other compound, so the combined organics were washed with saturated NaCl solution. TLC indicated that there was no by-product left, so the organics were dried over Na_2SO_4 and concentrated. The obtained brown oil was purified by trituration with DCM/LP 1:1 to get a colourless (**1b**) or slightly yellow (**1c**) solid; according to NMR in high purity.

3.2.2 Standard procedure (SP2) for the preparation of 2-Aminobenzamidoxime-adducts

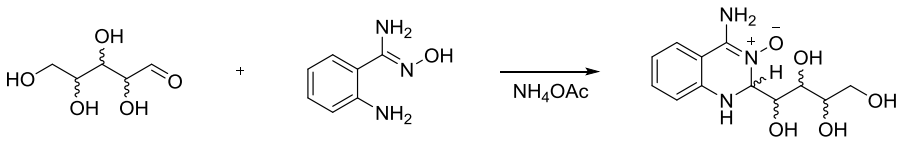

The corresponding sugar (3 mmol) was dissolved in NH_4OAc buffer (10 ml, 100 mM) and ABAO (3 mmol) was added. After stirring the solution overnight, it was washed with Et_2O and LP and the aqueous layer was evaporated *via* lyophilisation to yield the epimer mixtures, which were attempted to be further isolated by crystallisation or trituration.

3.3 Synthesis of 2-Aminobenzamidoxime-derivatives

3.3.1 2-Amino-5-nitro-benzamidoxime (1a)

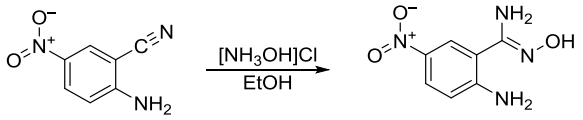

Ia **1a**

2-Bromo-5-nitrobenzonitrile (**Ia**, 18.81 mmol, 3.00 g) was dissolved in EtOH (48 ml). As it did not get dissolved at all, water (16 ml) was added, hydroxylamine hydrochloride (27.59 mmol, 1.92 g) and $NaHCO_3$ (33.10 mmol, 2.78 g) were added and the solution was refluxed overnight.

The next day, the solution had turned into a suspension. TLC (LP/EtOAc 1:2) of the supernatant fluid indicated that there was no starting material left and the reaction was complete.

The yellow solid was filtered and washed with EtOH/H_2O (3:1) and after solubility experiments that the solid is hardly soluble in iPrOH, it was washed portionwise with cold iPrOH to yield the expected structure **1a** in good purity according to NMR.

Analytical data in accordance with the literature[19].

Yield: 69 % (2.51 g, 12.79 mmol)

Appearance: yellow solid

Melting point: 221-223 °C (literature: 221-223 °C) [19]

TLC: R_f (LP/ EtOAc 1:2) = 0.66

^{1}H NMR (400 MHz, DMSO-d$_6$): δ 6.03 (s, 2H, -NH2 (Amidine)), 6.76 (d, *J* = 9.1 Hz, 1H, H3), 7.74 (s, 2H, -NH2), 7.93 (dd, *J* = 9.1, 2.6 Hz, 1H, H4), 8.36 (d, *J* = 2.6 Hz, 1H, H6), 9.91 (s, 1H, OH) ppm.

^{13}C NMR (101 MHz, DMSO): δ 113.0 (s, C1), 115.2 (s, C3), 125.1 (s, C6), 125.7 (s, C4), 135.8 (s, C5), 152.2 (s, Amidoxime), 153.5 (s, C2) ppm.

3.3.2 2-Amino-N-hydroxy-3-pyridinecarboximidamide (1b)

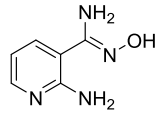

M = 152.16 g/mol

1b

According to SP1, 2-Amino-3-cyanopyridine **Ib** (1.50 g., 12.59 mmol), $[NH_3OH]Cl$ (1.31 g.18.81 mmol), and $NaHCO_3$ (1.90 g, 22.66 mmol) were converted into **1b**, which was obtained as a colourless solid and stored in a -20°C freezer.

Analytical data in accordance with the literature[10].

Yield: 83 % (1.59 g, 10.43 mmol)

Appearance: colourless solid

Melting point: 102-103 °C

TLC: R_f (DCM/MeOH 1:1) = 0.75

^{1}H NMR (400 MHz, DMSO-d_6): δ 5.86 (s, 2H, NH2 (Amidine)), 6.57 (dd, *J* = 7.6, 4.8 Hz, 1H, H5), 6.98 (s, 2H, NH2), 7.74 (dd, *J* = 7.7, 1.6 Hz, 1H, H4), 7.93 (dd, *J* = 4.8, 1.7 Hz, 2H, H6), 9.81 (s, 1H, OH) ppm.

^{13}C NMR (101 MHz, DMSO): δ 109.6 (s, C1), 111.7 (s, C5), 135.2 (s, C4), 148.3 (s, C6), 151.9 (s, Amidoxime), 157.1 (s, C2) ppm.

3.3.3 2-Aminobenzamidoxime (1c)

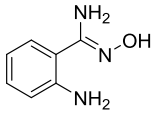

M = 151.17 g/mol

1c

According to TP1, 2-Amino-benzonitrile **Ic** (20.3 g., 171 mmol), $[NH_3OH]Cl$ (17.9 g, 257 mmol), and $NaHCO_3$ (26.0 g, 309 mmol) were converted into **1c**, which was obtained as a slightly yellow solid and stored in a -20°C freezer.

Analytical data in accordance with literature[19].

Yield: 80 % (20.6 g, 136.3 mmol)

Appearance: slightly yellow solid

Melting point: 83-84 °C (literature: 70-72 °C)[19]

TLC: R_f (LP/EtOAc 1:1) = 0.45

^{1}H NMR (400 MHz, DMSO-d_6): δ 5.71 (s, 2H, -NH2 (Amidine)), 6.20 (s, 2H, -NH2), 6.48 – 6.56 (m, 1H, H5), 6.64 – 6.68 (m, 1H, H3), 6.98 – 7.07 (m, 1H, H4), 7.33 – 7.39 (m, 1H, H6), 9.55 (s, 1H, OH) ppm.

^{13}C NMR (101 MHz, DMSO): δ 114.6 (s, C1), 115.3 (s, C5), 115.9 (s, C3), 127.7 (s, C6), 129.4 (s, C4), 147.2 (s, C2), 153.3 (s, Amidoxime) ppm.

3.4 Synthesis of 4-O-Formyl-2,3-O-isopropylidene-L-erythrose

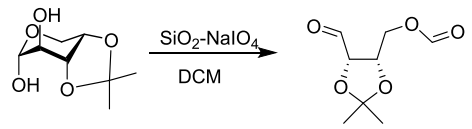

II **2**

4-O-Formyl-2,3-O-isopropylidene-L-erythrose was prepared according to the literature.[17]

Arabinose-acetonide **II** (0.284 mmol, 0.054 g) was taken up in dry DCM (1.1 mL) and under vigorous stirring SiO_2-$NaIO_4$ (0.568 mmol, 0.868 g) was added. The addition of some additional DCM kept the mixture stirrable. TLC analysis (LP/EtOAc 1:1) after 30 minutes indicated complete conversion of starting material to the targeted less polar material, with unreacted nonpolar by-product being visible.

The reaction mixture was filtered; the silica gel was washed with $CHCl_3$ and evaporated.

Analytical data in accordance with the literature.[17]

Yield: 26 % (13.8 mg, 0.074 mmol)

Appearance: colourless liquid

^{1}H NMR (600 MHz, D_2O): δ 1.42 (s, 3H, CH3), 1.51 (s, 3H, CH3), 4.20 (t, *J* = 7.0 Hz, 1H, H4), 4.31 (dd, *J* = 12.1, 7.8 Hz, 2H, H2 & H4), 4.52 – 4.60 (m, 1H, H3), 8.19 (s, 1H, OCHO) ppm.

3.5 Synthesis of ABAO-adducts

3.5.1 (R)-4-Amino-2-((1S,2S,3S)-1,2,3,4-tetrahydroxybutyl)-1,2-dihydroquinazoline 3-oxide

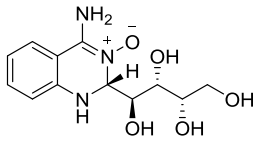

M = 283.28 g/mol

4

According to SP2, D-lyxose (0.407 g, 2.71 mmol) and ABAO (**1c**) (0.492 g, 3.26 mmol) were converted into **4**. An aliquot (100 mg) was purified which was obtained as a colourless solid and obtained in high purity according to NMR; it was stored in a -20°C freezer.

Yield: 38 % (38 mg, 0.134 mmol)

Appearance: colourless solid

Melting point: 209-211 °C

TLC: R_f (DCM/MeOH 1:1) = 0.31

^{1}H NMR (400 MHz, D_2O): δ 3.52 – 3.61 (m, 2H, H4'), 3.61 – 3.66 (m, 1H, H2'), 3.83 (t, *J* = 5.9 Hz, 1H, H3'), 4.05 (d, *J* = 9.5 Hz, 1H, H1'), 5.25 (s, 1H, H2), 6.75 (t, *J* = 8.6 Hz, 2H, H5/H8), 7.23 (t, *J* = 7.5 Hz, 1H, H6/H7), 7.32 (d, *J* = 7.7 Hz, 1H, H6/H7) ppm.

^{13}C NMR (101 MHz, D_2O): δ 63.0 (s, C4'), 68.8 (s, C2'), 69.9 (s, C3'), 70.4 (s, C1'), 73.5 (s, C2), 114.5, 118.3 (s, 2x C5/C8), 123.5, 133.1 (s, 2x C6/C7) ppm.

HR-MS:

HRMS (+ESI) m/z: calc. for $C_{12}H_{18}N_3O_5$ $[M+H]^+$: 284.1241, found: m/z = 284.1236

3.5.2 (R,S)-4-Amino-2-((1S,2R,3S)-1,2,3,4-tetrahydroxybutyl)-1,2-dihydroquinazoline 3-oxide

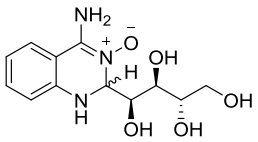

M = 283.28 g/mol

5

According to SP2, L-arabinose (0.103 g, 0.688 mmol) and ABAO (**1c**) (0.125 g, 0.826 mmol) were converted into **5**; the epimer ratio was 1:1 and was obtained in good purity according to NMR; it was stored in a -20°C freezer.

^{1}H NMR (400 MHz, D_2O)(epimer mixture): δ 3.60 – 3.65 (m, 1H, H4'), 3.68 (d, *J* = 3.0 Hz, 2H, H3'), 3.70 – 3.74 (m, 1H, H2'), 3.78 – 3.86 (m, 1H, H4'), 4.02 (d, *J* = 4.7 Hz, 0H, H1'), 4.13 (d, *J* = 5.0 Hz, 1H, H1'), 5.14 (t, *J* = 4.8 Hz, 1H, H2), 6.87 – 6.95 (m, 2H, H5/H8), 7.35 – 7.42 (m, 1H, H6/H7), 7.49 (d, *J* = 8.0 Hz, 1H, H6/H7) ppm.

^{13}C NMR (101 MHz, D_2O)(epimer mixture): δ 63.1 (d, *J* = 12.1 Hz (C4')), 68.6 (s, C1'), 69.6 (s, C3'), 70.7 (s, C2'), 72.3 (s, C1'), 74.6 (d, *J* = 9.7 Hz (C2)), 115.2, 115.6, 119.0, 119.4 (s, 4x C5/C8), 124.3 (d, *J* = 8.0 Hz), 134.0 (d, *J* = 9.9 Hz (2x C6/C7), ppm.

HR-MS:

HRMS (+ESI) m/z: calc. for $C_{12}H_{18}N_3O_5$ $[M+H]^+$: 284.1241, found: m/z = 284.1251

3.5.3 (R,S)-4-Amino-2-((1S,2R,3R)-1,2,3,4-tetrahydroxybutyl)-1,2-dihydroquinazoline 3-oxide

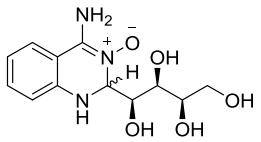

M = 283.28 g/mol

6

According to SP2, D-xylose (0.102 g, 0.678 mmol) and ABAO (**1c**) (0.123 g, 0.814 mmol) were converted into **6**. the epimer ratio was 1:1 and was obtained in good purity according to NMR; it was stored in a -20°C freezer.

^{1}H NMR (400 MHz, D_2O)(epimer mixture): δ 3.40 – 3.50 (m, 1H, H4'), 3.50 – 3.54 (m, 1H, H4'), 3.56 – 3.59 (m, 1H, H4'), 3.60 – 3.62 (m, 1H, H4'), 3.69 – 3.75 (m, 2H, H2',H3'), 3.79 (dd, *J* = 4.9, 2.0 Hz, 1H, H1'), 3.96 (t, *J* = 3.8 Hz, 1H, H1'), 5.09 (d, *J* = 4.1 Hz, 1H, H2), 6.75 – 6.84 (m, 2H, H5/H8), 7.26 – 7.32 (m, 1H, H6/H7), 7.37 – 7.43 (m, 1H, H6/H7) ppm.

^{13}C NMR (101 MHz, D_2O)(epimer mixture): δ 62.3 (d, *J* = 4.4 Hz (C4')), 70.3 (s, C1'), 70.6, 71.9 (s, 2x C2' & C3'), 73.4 (s, C1'), 74.0 (s, C2), 115.2 (s, C5/C8), 119.1 (d, *J* = 3.3 Hz(C5/C8),), 124.1, 124.3, 133.9, 134.0 (s, 4x C6/C7) ppm.

HR-MS:

HRMS (+ESI) m/z: calc. for $C_{12}H_{18}N_3O_5$ $[M+H]^+$: 284.1241, found: m/z = 284.1253

3.5.4 (R,S)-4-Amino-2-((1S,2S,3R)-1,2,3,4-tetrahydroxybutyl)-1,2-dihydroquinazoline 3-oxide

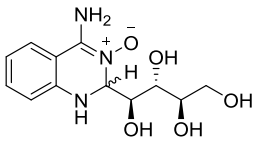

M = 283.28 g/mol

7

According to SP2, D-ribose (0.101 g, 0.672 mmol) and ABAO (0.122 g, 0.807 mmol) were converted into **7**. The epimer ratio was 1:3 and was obtained in good purity according to NMR; it was stored in a -20°C freezer.

^{1}H NMR (400 MHz, D_2O)(main isomer): δ 3.63 – 3.70 (m, 1H, H4'), 3.73 – 3.78 (m, 1H, H4'), 3.82 (dd, *J* = 8.7, 4.3 Hz, 1H, H2'), 3.87 – 3.93 (m, 1H, H3'), 4.08 – 4.13 (m, 1H, H1'), 5.31 (d, *J* = 2.0 Hz, 1H, H2), 6.81 – 6.92 (m, 2H, H5/H8), 7.32 – 7.39 (m, 1H, H6/H7), 7.41 – 7.49 (m, 1H, H6/H7) ppm.

^{13}C NMR (101 MHz, D_2O)(main isomer): δ 61.9 (s, C4'), 70.9, 71.1 (s, 2x C1'/C2'), 72.7 (s, C3'), 73.6 (s, C2), 114.8, 118.6 (s, 2x C5/C8), 124.0, 133.9 (s, 2x C6/C7).

HR-MS:

HRMS (+ESI) m/z: calc. for $C_{12}H_{17}N_3O_5$ $[M+Na]^+$: 306.1060, found: m/z = 306.1065

3.6 Representative time resolved ABAO-adduct formation

General remarks

Blank reactions were performed and involved in calculations. All reactions were performed in triplicates.

Sample preparation for plate reader

To 190 µl of a solution of ABAO (42.1 mM) dissolved in NH_4OAc buffer (100 mM, pH = 4.5) in a 96 well plate, 10 µl of sugar (80 mM) in H_2O was added.

The plate was shaken in the plate reader and measurements were conducted at 405 nm for specific time (usually 60-480 min). For the blank, addition of water (10 µl) instead of sugar solution was done. If multiple samples are measured, it is recommended to start pipetting with the sample which is expected to be the slowest one.

Fitting curve *via Prism* or *Excel*

The time resolved curve is fitted *via* prism by one phase association to obtain $k_{app.}$ To receive k_{app}, the calculation can be done by the software *Prism* or manually in *Excel*. With *Prism*, the corresponding time resolved curve of the measurement is analysed *via* the setting “one-phase association” which yields k_{app}. To get the total k, k_{app} is divided by the concentration of ABAO.

If *Prism* is not available, the calculation can also be done in *Excel*. The logarithm is taken of the highest value of the curve and is subtracted with those data points to get a straight line. Finally, the trendline formula shows k_{app} and the total k can again be received if k_{app} is divided by the concentration of ABAO used in the measurement.

3.7 Appendix

3.7.1 Crystal structure report of (R)-4-Amino-2-((1S,2S,3S)-1,2,3,4-tetrahydroxybutyl)-1,2-dihydroquinazoline 3-oxide

Bond precision: C-C = 0.0047 A Wavelength=1.54178

Cell: a=9.9685(5) b=5.3650(2) c=11.9561(6)

alpha=90 beta=101.567(4) gamma=90

Temperature: 100 K

	Calculated	Reported
Volume	626.44 (5)	626.44 (5)
Space group	P 21	P 21
Hall group	P 2yb	P 2yb
Moiety formula	C12H17N3O5	
Sum formula	C12H17N3O5	C12H17N3O5
Mr	283.29	283.28
Dx, g cm^{-3}	1.502	1.502
Z	2	2
Mu (mm^{-1})	0.999	0.999
F000	300.0	300.0
F000'	301.05	
H, k, lmax	12, 6, 14	12, 6, 14
Nref	2552 [1419]	2520
Tmin, Tmax	0.988, 0.990	0.603, 0.754
Tmin'	0.887	

Correction method= # Reported T Limits: Tmin=0.603 Tmax=0.754

AbsCorr = MULTI-SCAN

Data completeness= 1.78/0.99 Theta(max)= 74.289

R(reflections)= 0.0390 (2147) wR2(reflections)= 0.1005 (2520)

S = 1.049 Npar= 209

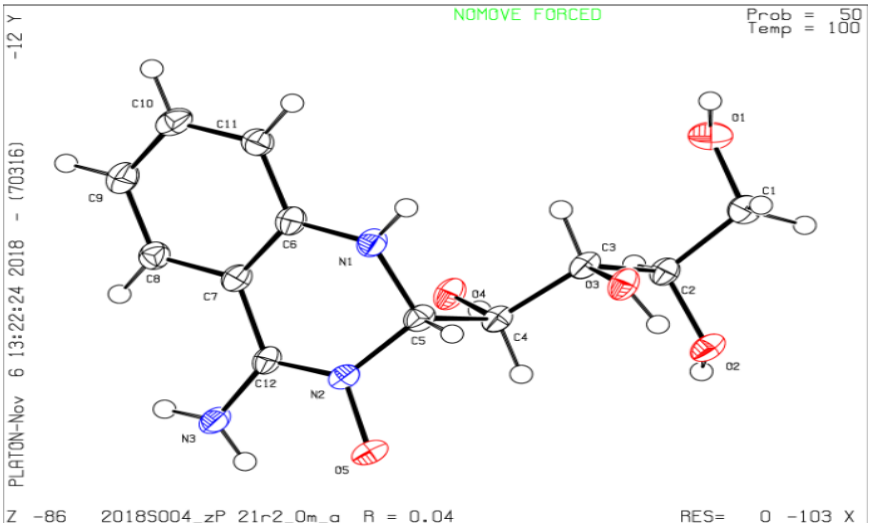
NOMOVE FORCED
Prob = 50
Temp = 100
-12 Y
PLATON-Nov 6 13:22:24 2018 - (70316)
C10
C11
C9
C6
N1
C8
C7
C12
N2
N3
O5
C5
O4
C4
C3
O3
C2
O1
C1
O2
Z -86 2018S004_zP 21r2_0m_a R = 0.04
RES= 0 -103 X

4 References

[1] Fletcher, H. G. Augustin-Pierre Dubrunfaut—An early sugar chemist. *Journal of Chemical Education* **1940**, *17*, 153.

[2] Isbell, H. S.; Hudson, C. S. The course of the oxidation of the aldose sugars by bromine water. *Bureau of Standards Journal of Research* **1932**, *8*, 327-338.

[3] Haga, H.; Nakajima, T. Analysis of aldoses and alditols by capillary gas chromatography as alditol trifluoroacetates. *Chemical & Pharmaceutical Bulletin* **1988**, *36*, 1562-1564.

[4] Varma, R.; French, D. Mechanism of the cyanohydrin (Kiliani-Fischer) synthesis. *Carbohydrate Research* **1972**, *25*, 71-79.

[5] Adjé, N.; Vogeleisen, F.; Uguen, D. Improved conditions for the Kiliani-Fischer synthesis. *Tetrahedron Letters* **1996**, *37*, 5893-5896.

[6] Ruff, O. Ueber die Verwandlung der d-Gluconsäure in d-Arabinose. *Berichte der deutschen chemischen Gesellschaft* **1898**, *31*, 1573-1577.

[7] Stapley, J. A.; BeMiller, J. N. The Ruff degradation: a review of previously proposed mechanisms with evidence that the reaction proceeds by a Hofer–Moest-type reaction. *Carbohydrate Research* **2007**, *342*, 407-418.

[8] Angyal, S. J. The Composition of Reducing Sugars in Solution. *Advances in Carbohydrate Chemistry and Biochemistry* **1984**, *42*, 15-68.

[9] Dworkin, J. P.; Miller, S. L. A kinetic estimate of the free aldehyde content of aldoses. *Carbohydrate Research* **2000**, *329*, 359-365.

[10] Kitov, P. I.; Vinals, D. F.; Ng, S.; Tjhung, K. F.; Derda, R. Rapid, hydrolytically stable modification of aldehyde-terminated proteins and phage libraries. *Journal of the American Chemical Society* **2014**, *136*, 8149-8152.

[11] Ott, G. R.; Anzalone, A. V. Synthetic studies toward 3-(acylamino)-1H-indazoles and development of a one-pot, microwave-assisted, oxadiazole condensation/Boulton-Katritzky rearrangement. *Synlett* **2011**, *20*, 3018-3022.

[12] Abstracts. *Journal of North Carolina Academy of Science* **2012**, *128*, 108-143.

[13] Serianni, A. S.; Clark, E. L.; Barker, R. Carbon-13-enriched carbohydrates. Preparation of erythrose, threose, glyceraldehyde, and glycolaldehyde with

13C-enrichment in various carbon atoms. *Carbohydrate Research* **1979**, *72*, 79-91.

[14] Angyal, S.; Wheen, R. The composition of reducing sugars in aqueous solution : glyceraldehyde, erythrose, threose. *Australian Journal of Chemistry* **1980**, *33*, 1001-1011.

[15] Drew, K. N.; Zajicek, J.; Bondo, G.; Bose, B.; Serianni, A. S. 13C-labeled aldopentoses: detection and quantitation of cyclic and acyclic forms by heteronuclear 1D and 2D NMR spectroscopy. *Carbohydrate Research* **1998**, *307*, 199-209.

[16] Zhu, Y.; Zajicek, J.; Serianni, A. S. Acyclic Forms of [1-13C]Aldohexoses in Aqueous Solution: Quantitation by 13C NMR and Deuterium Isotope Effects on Tautomeric Equilibria. *The Journal of Organic Chemistry* **2001**, *66*, 6244-6251.

[17] Draskovits, M.; Stanetty, C.; Baxendale, I. R.; Mihovilovic, M. D. Indium- and Zinc-Mediated Acyloxyallylation of Protected and Unprotected Aldotetroses—Revealing a Pronounced Diastereodivergence and a Fundamental Difference in the Performance of the Mediating Metal. *The Journal of Organic Chemistry* **2018**, *83*, 2647-2659.

[18] Gottlieb, H. E.; Kotlyar, V.; Nudelman, A. NMR Chemical Shifts of Common Laboratory Solvents as Trace Impurities. *The Journal of Organic Chemistry* **1997**, *62*, 7512-7515.

[19] Lin, C.-C.; Hsieh, T.-H.; Liao, P.-Y.; Liao, Z.-Y.; Chang, C.-W.; Shih, Y.-C.; Yeh, W.-H.; Chien, T.-C. Practical synthesis of N-substituted cyanamides via tiemann rearrangement of amidoximes. *Organic Letters* **2014**, *16*, 892-895.